

Supporting Information:

Computer Vision Uncovers Predictors of Physical Urban Change

Nikhil Naik*, Scott Duke Kominers, Ramesh Raskar, Edward L. Glaeser, and César A. Hidalgo

Contents

1. Data and Methods	1
1.1. The Street View Image Dataset	1
1.2. Image Feature Extraction	2
1.3. Removal of Unsuitable Images	2
1.4. Streetchange Calculation	3
1.5. Removing Erroneous Pairs	4
1.6. Image Quality and Streetchange	5
1.7. Validating Streetchange	5
1.8. Streetscore: Generalization Performance	7
2. Regressions	7
2.1. Do Social Characteristics Predict Changes in Streetscore?	8
2.2. The Filtering Hypothesis of Urban Change	8
3. Additional Examples and Map Visualizations	8

1. Data and Methods

Using a dataset consisting of human-coded image comparisons, we train a computer vision algorithm to predict perceived safety of individual street scenes (“Streetscore”); we then obtain “Streetchange” by comparing that measurement across Street View images of the same locations from 2007 (the “2007 image”) and 2014 (the “2014 image”).

1.1. The Street View Image Dataset

We first describe the Street View image dataset used in this paper. We obtained 360° panorama images of streetscapes from five US cities using the Google Street View Application Programming Interface (API). Each panorama was associated with a unique identifier (“panoid”), latitude, longitude, and time stamp (which specified

*E-mail: naik@fas.harvard.edu

the month and year of image capture). We extracted an image cutout from each panorama by specifying the heading and pitch of the camera relative to the Street View vehicle. We obtained a total of 1,645,760 image cutouts for street blocks in Baltimore, Boston, Detroit, New York, and Washington DC, captured in years 2007 (the “2007 panel”) and 2014 (the “2014 panel”). For the street blocks that lack images for either 2007 or 2014, we completed the “2007” and “2014” panels using images from the closest years for which data was available. As a result, 5% of the images in the “2007” panel are from either 2008 or 2009. Similarly, 12% of the images in the “2014” panel are from 2013. We matched image cutouts from the 2007 and 2014 panels by using their geographical locations (i.e. latitude and longitude) and by choosing the same heading and pitch. This process gave us images that show the same place, from the same point of view, but in different years. A large majority of images in our dataset were captured between the months of April and August, to avoid a change of season between the two images of the same location.

Next, we describe the computer vision algorithm used for obtaining Streetchange—a measure for physical urban change—from the 2007 and 2014 image panels.

1.2. Image Feature Extraction

Our computer vision algorithms work with a number of structured and unstructured features of the image data: First, we used the Geometric Layout algorithm [1] to assign pixel-wise semantic labels in four geometric classes: “ground,” “buildings,” “trees,” and “sky.” Next, we extracted two different image features separately for the pixels of the four geometric classes:

- We generated a texton dictionary [2] by convolving the images with a Gaussian filter bank and clustering their responses together; every pixel was then assigned to the nearest cluster center, creating a texton map. We computed 512-dimensional histograms with texton maps of the four geometric classes. We call this feature Geometric Texton Histograms (GTH).
- We calculated the GIST feature descriptor [3]—a global image feature that provides a low-dimensional representation of the spatial layout properties of a scene—for each of the geometric classes.

1.3. Removal of Unsuitable Images

A small number of Street View image pairs in the sample were unsuitable for comparison. In particular: some images were over-exposed, out of focus, or blurred; others had significant changes in greenery coverage likely driven by seasonal changes rather than urban foliage improvements. To eliminate these unsuitable pairs, we used a series of automated data cleaning methods:

- First, we removed over-exposed images, which typically result from the sun shining directly into the camera. To identify over-exposed pixels, we converted each image to the CIELAB color space, in which the L channel represents lightness and a, b channels represent the color. The color channels were combined as $C = (a, b)^T$. We computed an over-exposure value \mathcal{M} (between 0 and 1) at each pixel following methods introduced by Guo et al. [4]: At pixel i ,

$$\mathcal{M}_i = \frac{1}{2} \cdot \tanh \left(\delta \cdot \left((L_i - L_T) + (C_T - \|C_i\|_2) \right) \right),$$

with the constants set to $\delta = 1/60$, $L_T = 80$, and $C_T = 40$. We obtained the mean $\mathcal{M}_i^{\text{sky}}$ of \mathcal{M}_i over all the pixels that belonged to the “sky” geometric class, as predicted by the Geometric Layout algorithm [1]. We discarded the image pairs in which at least one of the images i had $\mathcal{M}_i^{\text{sky}} > 0.85$, indicating over-exposure. We discarded all image pairs containing at least one over-exposed image.



Figure S1. The Streetchange algorithm is robust to large weather and seasonal changes. In this example, our algorithm assigns a small Streetchange value to the image pairs, even though there is a drastic change in weather between the two images. Images courtesy of Google, Inc.

- Second, we removed images that were out-of-focus or contained motion blur. To detect such images, we computed the Absolute Central Moment (ACMO) of each image, a statistical measure that allows a simultaneous optimization of both focus and exposure [5]. If the normalized value of ACMO was less than 0.2, we labeled the image as blurred. We discarded all image pairs containing at least one blurred image.
- Finally, we discarded all image pairs in which the number of pixels in the image occupied by the “tree” object class (again, as predicted by the Geometric Layout algorithm [1]) changed by more than 10% between the 2007 image and the 2014 image. This process eliminated image pairs in which only one of the images had significant occlusion of buildings by trees.

1.4. Streetchange Calculation

Having removed the images unsuitable for urban change detection, we predicted the “Streetscores” of the remaining images using a support vector regression model trained with computer vision features and aggregate scores obtained from the crowdsourced study by Salesses et al. [6], as described next.

Salesses et al. [6] created an online crowdsourced game in which participants were shown images of streetscapes randomly chosen from New York, Boston, Linz and Salzburg. Participants were asked to choose one of the two images in response to three questions: “Which place looks safer?”, “Which place looks more upper class?”, and “Which place looks unique?”. In the Salesses et al. [6] study, 7,872 unique participants from 91 countries provided 186,188 comparisons (“clicks”) of image pairs drawn from a pool of 4,109 images for the question “Which place looks safer?”

Following Naik et al. [7], we converted the 186,188 pairwise comparisons for the question “Which place looks safer?” to ranked scores using a Bayesian ranking algorithm called Trueskill [8]. We call the Trueskill perceived safety score for each image that image’s *Streetscore*; these images’ Streetscores are “true scores” derived from aggregations of human assessments. We used the Streetscores obtained from human assessments to train a machine learning model that uses the GTH and GIST features of the corresponding images (described in Section 1.2) to predict how humans would score the perceived safety of Street View images. As we are only seeking to predict

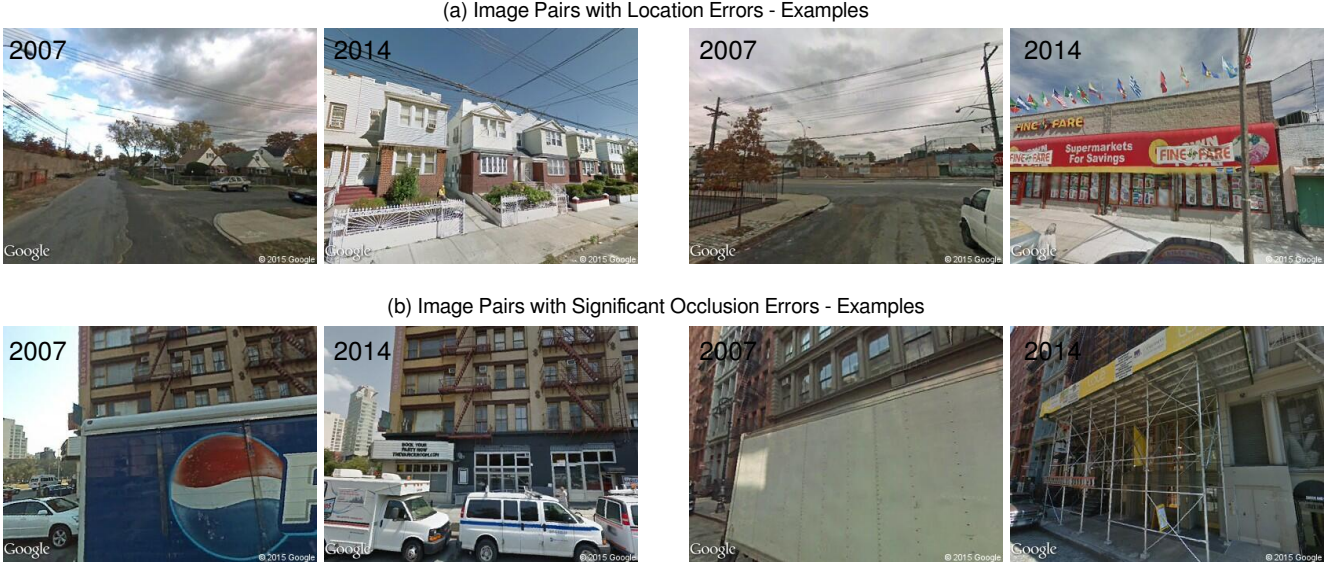


Figure S2. A human operator eliminated the small fraction of invalid image pairs containing location-coding errors or significant occlusion of buildings by large vehicles. Images courtesy of Google, Inc.

the human perception of American cities, we restricted the training sample to the 2,920 human-coded images from New York and Boston.

We used ν -Support Vector Regression (ν -SVR) [9] to predict image Streetscores. Given a set of training images with feature vectors \mathbf{x} and Streetscores $q \in \mathbb{R}$, ν -SVR with a linear kernel generates a weight vector \mathbf{w} and a bias term b under a set of constraints. The two variables (\mathbf{w}, b) are used to predict the Streetscore for a new image with feature vector \mathbf{x}' by evaluating $q' = \mathbf{w} \cdot \mathbf{x}' + b$. We measured the accuracy of our predictor using the Coefficient of Determination (R^2). We obtained $R^2 = 0.57$ over fivefold cross-validation on the training set.

In this paper we dropped the Geometric Color Histogram (GCH) features used by Naik et al. [7], since GCH features were more sensitive to weather changes than GIST and texton histograms. Dropping the GCH features, however, did not substantially reduce the predictor accuracy—the R^2 dropped from 0.5884 to 0.5709.

Next, we used the Streetscore predictor to calculate urban change from image pairs. As our predictor is a weight vector trained using image features on top of the four geometric classes (ground, building, trees and sky), we were able to compute the contribution of each geometric class to the Streetscore of each image. We chose to discard the contribution of the “trees” and “sky” classes since their scores depend on the season and weather at the time of image capture. Note that the “trees” class contains only large trees (and not landscaping), allowing us to account for changes in the built environment due to landscaping as part of the “ground” class. Figure S1 shows examples of image pairs with large weather and seasonal changes which have been accurately scored by our algorithm.

After computing the Streetscore for each image in a 2007–2014 image pair, we calculated “Streetchange” as the difference between the 2014 image’s Streetscore and the 2007 image’s Streetscore.

1.5. Removing Erroneous Pairs

While we were able to computationally eliminate pairs containing over-exposed, blurred, or occluded images, we discovered two additional sources of error that made a small number of image pairs invalid for Streetchange calculation. The first source of error was incorrect location information for one or both images in an image pair. For these images, the geographic coordinates (latitude and longitude) obtained from Google Street View did not



Figure S3. The Streetchange algorithm is robust to the change in Street View image quality between years 2007 and 2014. Images courtesy of Google, Inc.

match with the actual geographic coordinates of the locations at which the images were captured (Figure S2-(a)). The second source of error was partial or complete occlusion of buildings by large vehicles (Figure S2-(b)), which were not removed by the procedure described in Section 1.3.

Our algorithm calculated a large positive or negative Streetchange value for image pairs containing location-coding or vehicle-occlusion errors, since the two images in such pairs look very different (Figure S2). Due to large variation in visual appearance within and across image pairs that contained these errors, we were unable to automatically eliminate such image pairs with a computer vision algorithm. Therefore, a human operator observed image pairs whose Streetchange value was larger than four standard deviations of change in Streetscore (which amounted to only 1,849 image pairs out of a total of 822,880—less than 0.23% of the sample). The operator manually eliminated image pairs which contained location-coding errors or vehicle-occlusion errors.

1.6. Image Quality and Streetchange

We also note that there is a difference in image quality between Street View images captured in year 2007 and Street View images from year 2008 or after (due to improvements in Google’s imaging hardware). But the Streetchange algorithm is robust to change in image quality from 2007 and 2014 (Figure S3) for a few reasons. First, a significant fraction of images in the training set are also from 2007, which helps to mitigate the effect of change in image quality. Second, we process the images at a resolution of 400×300 pixels; the difference in quality is not significant at this resolution. Finally, a higher fraction of 2007 Street View images (as compared to year 2014) tend to be over-exposed; but we discard such images from our calculations.

1.7. Validating Streetchange

We validated our final Streetchange measures using three sources: a survey on Amazon Mechanical Turk (AMT), a survey of graduate students in MIT’s School of Architecture and Planning, and data from Boston’s Planning and Development Authority.

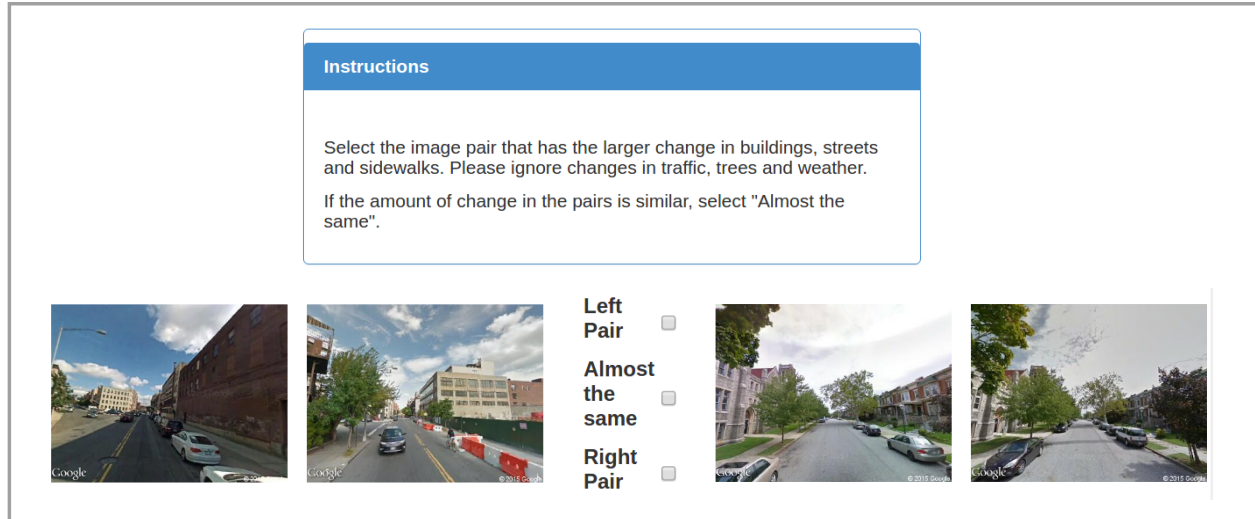


Figure S4. Screenshot of the Amazon Mechanical Turk experimental interface used for validating Streetchange. Insets courtesy of Google, Inc.

Validation with human observers: For the validation experiment on AMT, we selected 1,565 image pairs (roughly 1% of the final sample) using inverse transform sampling on Streetchanges. We presented AMT workers with two image pairs side-by-side (Figure S4) drawn randomly from the 1,565 image pairs and asked the following question:

Select the image pair that has the larger change in buildings, streets and sidewalks. Please ignore changes in traffic, trees and weather. If the amount of change in the pairs is similar, select “Almost the same”.

We obtained 28,170 pairwise comparisons for the 1,565 image pairs from 116 users—36 pairwise comparisons on average. We converted these pairwise comparisons to ranked scores using the Microsoft Trueskill algorithm [8]. Trueskill converges to a stable estimate of ranked scores after 12–36 comparisons, so we had enough comparisons to obtain accurate scores. We call this score *AMT–Streetchange*. A higher value of *AMT–Streetchange* is indicative of a larger absolute physical change in the image pair, as observed by the AMT users.

Next, we obtained binned ranks between 1 and 30 for both *AMT–Streetchange* and the absolute value of *Streetchange* output of our algorithm. Comparing the two, we found a Spearman’s rank correlation of 0.72 ($p < 1 \times 10^{-5}$) between them. These results indicate that the algorithm outputs on Streetchanges are consistent with human judgments on changes in urban environment.

For the validation experiment with graduate students in MIT’s School of Architecture and Planning, we presented the students (number of participants = 3) with 100 image pairs, where 50 image pairs contained large negative Streetchange and 50 image pairs contained large positive Streetchange. We asked them to choose if the image pair shows signs of positive change, negative change, or no change, and aggregated their responses with a majority rule. The students agreed with positive Streetchange (as scored by our algorithm) for 88% of the image pairs and they agreed with negative Streetchange for 59% of the image pairs. The lower agreement in the negative change was a result of students classifying demolition of blighted properties as a positive change (while our algorithm tends to classify them as negative).

Table S1. Summary Statistics for the Boston Validation Experiment (Section 1.7) (N = 222)

Variables	Description	Mean	SD	Min	Max
Streetchange 2007–2014	Mean Streetchange 2007–2014 of all sampled street blocks within a census tract	1.290	0.509	-1.599	2.613
Log Total Square Footage 2012–2014	Total square footage built per square mile within a census tract	13.527	1.548	10.109	17.202

Table S2. Streetscore: Generalization Performance (R^2)

Test Train	New York	Boston
New York	0.5399	0.5033
Boston	0.5028	0.5384

Validation with infrastructure development data: In the third validation experiment, we tested the relationship between improvements in Streetscore and improvements in infrastructure, using data on new developments in Boston (for summary statistics, see Table S1). We collected data on all public and private building projects from the Boston Planning and Development Agency (BPDA). We computed the total new square footage built per square mile for each census tract during the period 2012–2014 and tested its relationship with Streetchange 2007–2014. We expect census tracts where more square footage was built during 2012–2014 to be associated with a higher Streetchange, due to the physical improvements in these neighborhoods between the 2007 and 2014 image panels. And indeed, we find that infrastructure improvements are positively and significantly associated to Streetchange—one standard deviation increase in log total square footage corresponds to roughly half a standard deviation increase in Streetchange. We estimate:

$$\text{Streetchange } 2007 - 2014 = \frac{1.620}{(0.069)} + \frac{0.159^{***}}{(0.035)} \cdot \text{Log total square footage} \quad (1)$$

These results provide empirical evidence for the connection between improvements in Streetscore and improvements in infrastructure.

1.8. Streetscore: Generalization Performance

Computer vision algorithms might have difficulty generalizing to out-of-sample data. Since we compute Streetscores for images from Baltimore, Detroit, and Washington DC using an algorithm trained with images from Boston and New York, we would like to estimate whether the Streetscore predictor can generalize without a significant drop in accuracy. So we performed an experiment where we trained a Streetscore predictor using images just from New York and measured the accuracy of its predictions on Boston images in our dataset, and vice versa. We found that the R^2 drops by only 0.036 on average during cross-city prediction (Table S2).

2. Regressions

We calculated Streetchange for 2007–2014 image pairs sampled uniformly from Baltimore, Boston, Detroit, New York, and Washington DC. Using tract boundaries from the 2010 US Census, we aggregated 2007 Streetscore and 2007–2014 Streetchange across each census tract. We obtained census tract characteristic data from the 2000 US Census, adjusted to the 2010 census tract boundaries [10]. For summary statistics, see Table S3.

2.1. Do Social Characteristics Predict Changes in Streetscore?

We now present the cross-sectional demographic and economic correlates of the 2007 Streetscore and 2007–2014 Streetchange (Table S4). For each census tract, we considered the following socioeconomic indicators from the 2000 US Census: population density, level of education, median income, housing price and rental costs, housing vacancy, race, and poverty. We find that the socioeconomic characteristics that best predict higher Streetscore in 2007—density and education—are also the best predictors of increases in Streetscore between 2007 and 2014. These relationships hold regardless of whether we control for the 2007 Streetscore or other variables. We find that other variables, such as income, housing prices, rent, race, and poverty have little or no predictive power in our context.

2.2. The Filtering Hypothesis of Urban Change

In addition to the invasion and tipping hypotheses of urban change discussed in main text, we evaluated the filtering hypothesis [11] of urban change. The filtering hypothesis suggests cycles in which neighborhoods gradually decay until they get upgraded. To test the hypothesis that building age shapes streetscape change, we regressed the 2007 Streetscore and 2007–2014 Streetchange on the shares of the building stock (as of the year 2000) built during different decades. The data grouped together all buildings erected before 1939. There is weak support for the filtering hypothesis in our dataset (Table S5): we found that neighborhoods with newer housing stocks score higher than neighborhoods built in the 1950s. However, we cannot rule out the possibility that our finding is also reflective of differences in the perception of various architectural styles, as neighborhoods built before 1939 (prior to the widespread adoption of modernist architecture in the US) also score highly.

3. Additional Examples and Map Visualizations

Figures S5–S7 present additional examples of positive Streetchange from the five cities in our dataset. The examples show that Streetchange is able to detect both upgrading and new construction. Figure S8 shows additional examples of negative Streetchange, which are associated with urban blight and decline in upkeep.

Figures S9–S28 present map visualizations for Log Population Density 2000, Share College Education 2000, Streetscore 2007, and Streetchange 2007–2014 for the five cities in our dataset.

References

- [1] Hoiem D, Efros AA, Hebert M (2008) Putting objects in perspective. *International Journal of Computer Vision* 80(1):3–15.
- [2] Malik J, Belongie S, Leung T, Shi J (2001) Contour and texture analysis for image segmentation. *International Journal of Computer Vision* 43(1):7–27.
- [3] Oliva A, Torralba A (2001) Modeling the shape of the scene: A holistic representation of the spatial envelope. *International Journal of Computer Vision* 42(3):145–175.
- [4] Guo D, Cheng Y, Zhuo S, Sim T (2010) Correcting over-exposure in photographs. *IEEE Conference on Computer Vision and Pattern Recognition* pp. 515–521.
- [5] Shirvaikar MV (2004) An optimal measure for camera focus and exposure. *Southeastern Symposium on System Theory* pp. 472–475.
- [6] Salesses P, Schechtner K, Hidalgo CA (2013) The collaborative image of the city: Mapping the inequality of urban perception. *PLoS One* 8(7):e68400.

- [7] Naik N, Philipoom J, Raskar R, Hidalgo CA (2014) Streetscore – Predicting the perceived safety of one million streetscapes. *IEEE Conference on Computer Vision and Pattern Recognition Workshops* pp. 793–799.
- [8] Herbrich R, Minka T, Graepel T (2006) Trueskill: A Bayesian skill rating system. *Advances in Neural Information Processing Systems* pp. 569–576.
- [9] Schölkopf B, Smola AJ, Williamson RC, Bartlett PL (2000) New support vector algorithms. *Neural Computation* 12(5):1207–1245.
- [10] Logan JR, Xu Z, Stults BJ (2014) Interpolating US decennial census tract data from as early as 1970 to 2010: A longitudinal tract database. *The Professional Geographer* 66(3):412–420.
- [11] Margolis SE (1982) Depreciation of housing: An empirical consideration of the filtering hypothesis. *Review of Economics and Statistics* 64(1):90–96.

Table S3. Summary Statistics ($N = 2513$)

Variables	Description	Mean	SD	Min	Max
Streetscore 2007	Mean Streetscore 2007 of all sampled street blocks within a census tract	7.757	2.587	1.681	18.93
Streetchange 2007–2014	Mean Streetchange 2007–2014 of all sampled street blocks within a census tract	1.39	0.779	-4.076	6.121
Log Population Density 2000	Log of population density within a census tract	-4.655	1.22	-15.29	-2.48
Share College Education 2000	Share of adults with a four-year college degrees within a census tract	0.254	0.216	0	1
Log Median Income 2000	Log of median income of adults within a census tract	4.54	0.206	3.884	5.276
Log Monthly Rent 2000	Log of median monthly rent within a census tract	6.40	0.390	4.595	7.601
Log Housing Price 2000	Log of median housing price within a census tract	5.223	0.311	3.938	6
Poverty Rate 2000	Share of households under poverty line within a census tract	0.218	0.137	0	1
Share African-American 2000	Share of African-Americans within a census tract	0.366	0.371	0	1
Share Hispanic 2000	Share of Hispanics within a census tract	0.192	0.221	0	0.927
Share Vacant Units 2000	Share of vacant units within a census tract	0.036	0.055	0	0.348
Share Built 1990-2000	Share of housing stock built during 1990-2000 within a census tract	0.587	0.874	0	1
Share Built 1980-1989	Share of housing stock built during 1980-1989 within a census tract	0.404	0.573	0	0.659
Share Built 1970-1979	Share of housing stock built during 1970-1979 within a census tract	0.694	0.744	0	0.719
Share Built 1960-1969	Share of housing stock built during 1960-1969 within a census tract	0.123	0.983	0	1
Share Built 1950-1959	Share of housing stock built during 1950-1959 within a census tract	0.164	0.105	0	0.748
Share Built 1940-1949	Share of housing stock built during 1940-1949 within a census tract	0.171	0.956	0	0.815
Share Built before 1940	Share of housing stock built before 1940 within a census tract	0.394	0.201	0	1

All socioeconomic variables are from the 2000 US Census. Streetscore 2007 and Streetchange 2007–2014 are computed using the method described in Section 1 of this document. All data are aggregated at the census tract level.

Table S4. Relationship Between Social Characteristics and Changes in Streetscore

Independent Variables	Coefficient	
	Streetscore 2007	Streetchange 2007–2014
Share College Education 2000	2.024*** (0.483)	1.099*** (0.162)
Log Population Density 2000	0.765*** (0.097)	0.080*** (0.026)
Log Median Income 2000	0.186 (0.920)	-0.118 (0.242)
Log Monthly Rent 2000	1.191*** (0.260)	-0.149 (0.096)
Log Housing Price 2000	0.986*** (0.274)	0.175* (0.090)
Poverty Rate 2000	3.815*** (1.114)	0.300 (0.312)
Share African-American 2000	0.151 (0.225)	-0.002** (0.001)
Share Hispanic 2000	0.878** (0.365)	0.312*** (0.118)
Share Vacant Units 2000	0.917*** (0.158)	0.090*** (0.033)
Streetscore 2007		-0.012 (0.013)

All models control for city fixed effects.

*** $p < 0.01$, ** $p < 0.05$, * $p < 0.1$

Standard errors corrected for spatial correlation are in parentheses. Regressions are estimated with a constant that is not reported.

Table S5. Evidence of Filtering

Independent Variables	Coefficient	
	Streetscore 2007	Streetchange 2007–2014
Share Built 1990-2000	4.390*** (1.422)	0.410 (0.341)
Share Built 1980-1989	4.638*** (1.406)	0.677* (0.346)
Share Built 1970-1979	2.077** (0.948)	0.079 (0.259)
Share Built 1960-1969	2.367** (1.119)	0.343 (0.288)
Share Built 1940-1949	-0.195 (1.227)	-0.720** (0.324)
Share Built Before 1940	4.614*** (0.618)	0.323* (0.194)
Streetscore 2007		0.000 (0.014)
Log Population Density 2000		0.106*** (0.033)
Share College Education 2000		0.648*** (0.106)

All models control for city fixed effects.

* * * $p < 0.01$, ** $p < 0.05$, * $p < 0.1$

Standard errors corrected for spatial correlation are in parentheses. Regressions are estimated with a constant that is not reported.

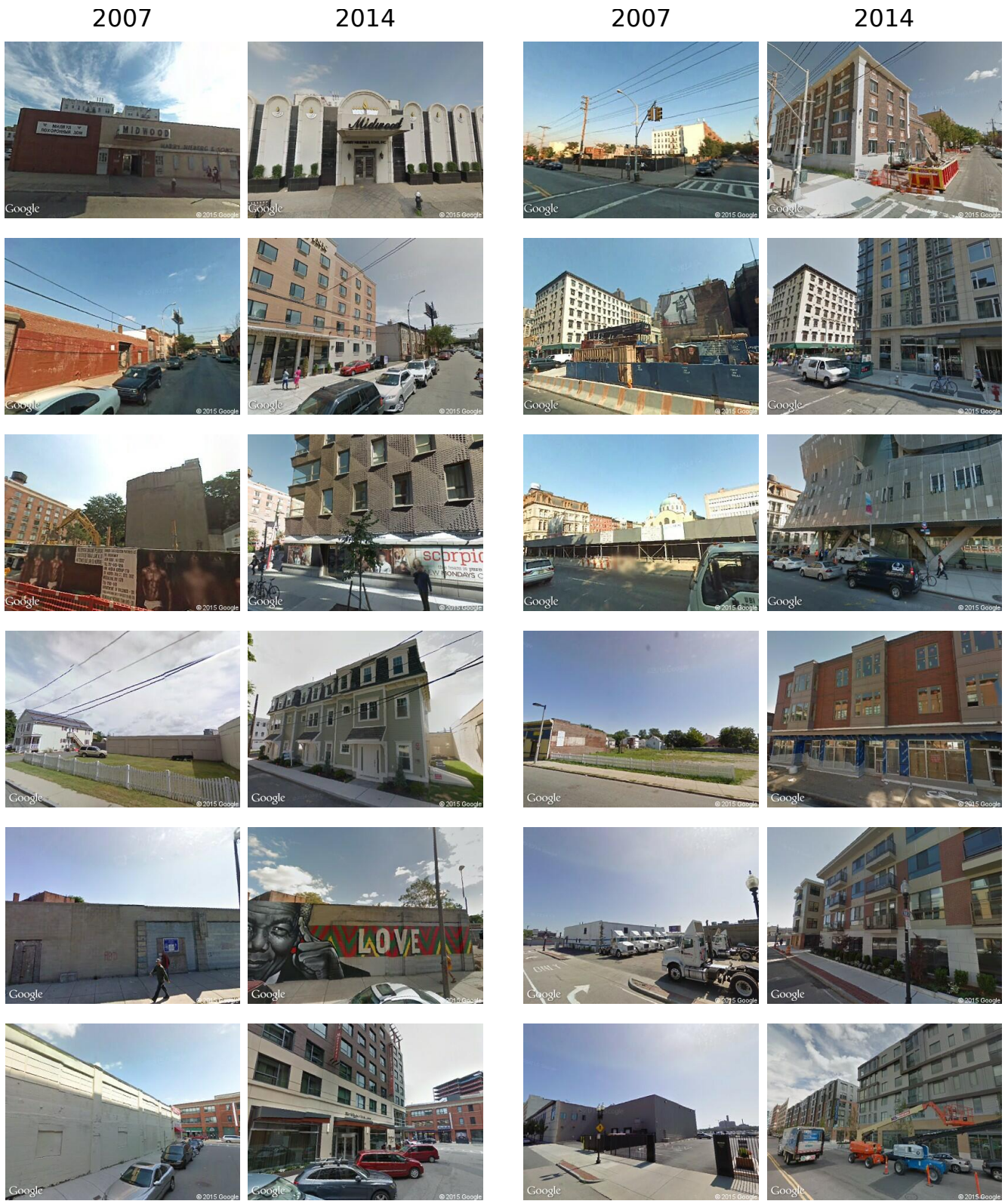


Figure S5. Additional examples of positive Streetchange. The first three rows show examples from New York City. The next three rows show examples from Boston. Images courtesy of Google, Inc.

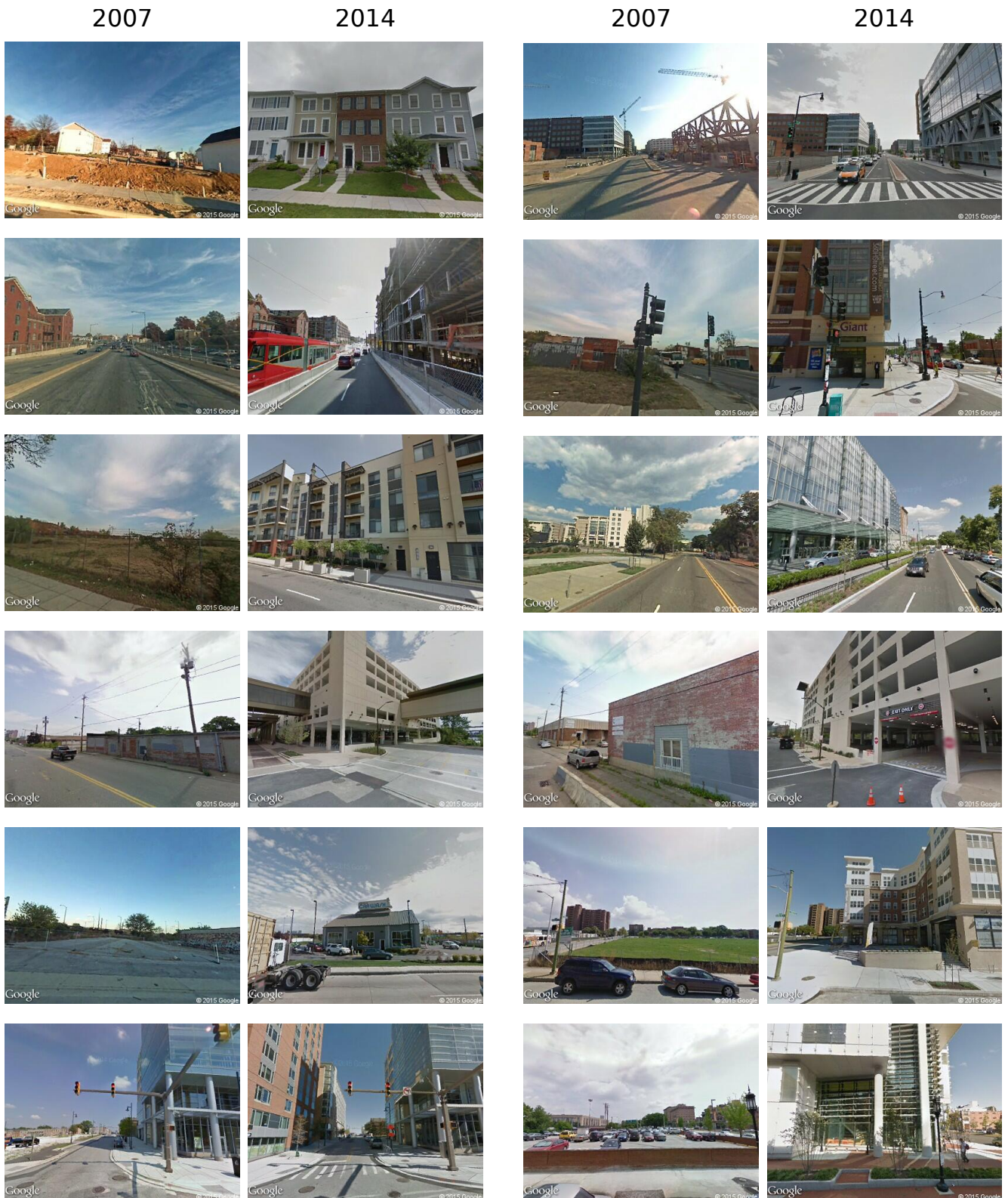


Figure S6. Additional examples of positive Streetchange. The first three rows show examples from Washington DC. The next three rows show examples from Baltimore. Images courtesy of Google, Inc.



Figure S7. Additional examples of positive Streetchange. All examples from Detroit. Images courtesy of Google, Inc.



Figure S8. Additional examples of negative Streetchange from the five cities in our dataset. Images courtesy of Google, Inc.

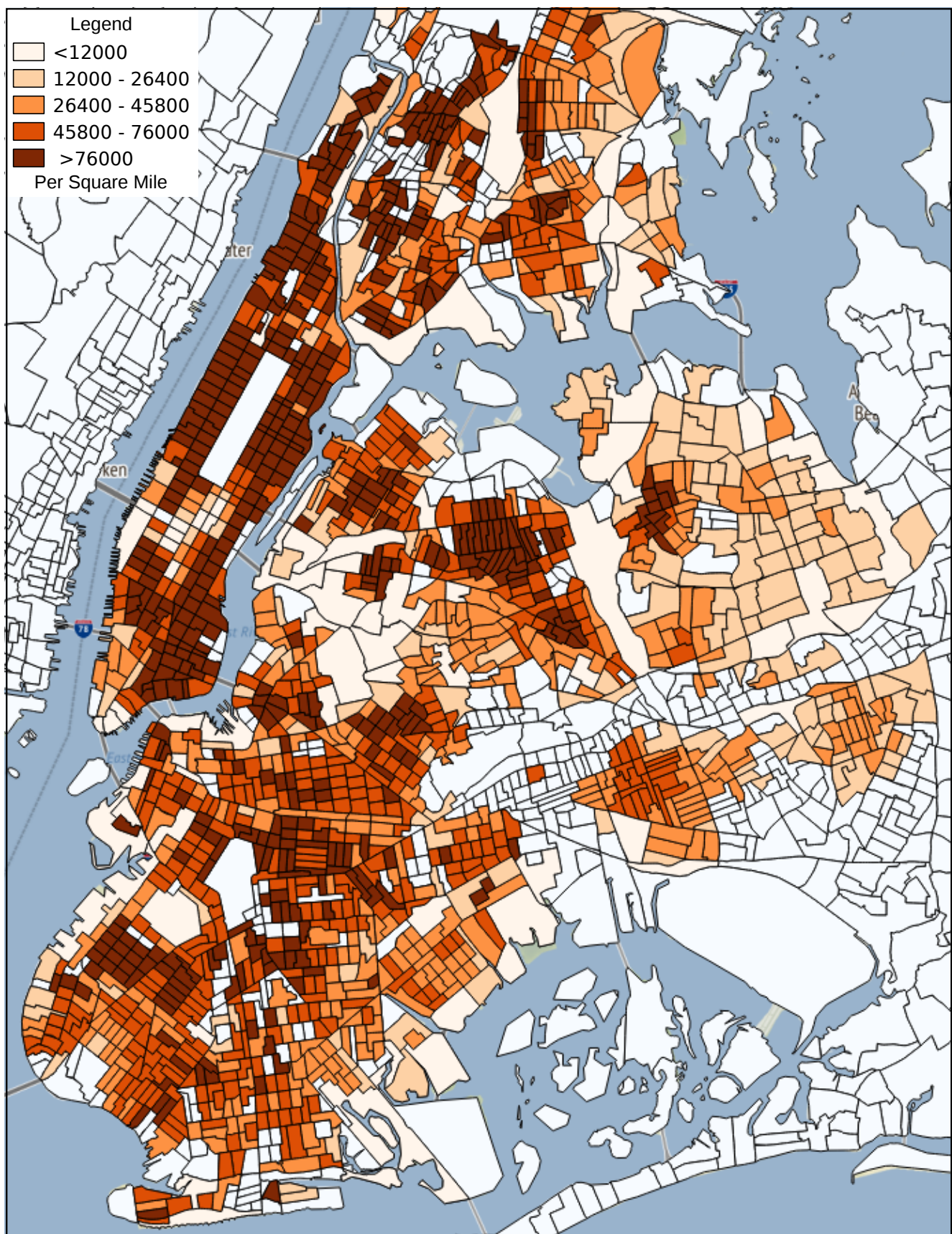


Figure S9. New York City: Log Population Density 2000.

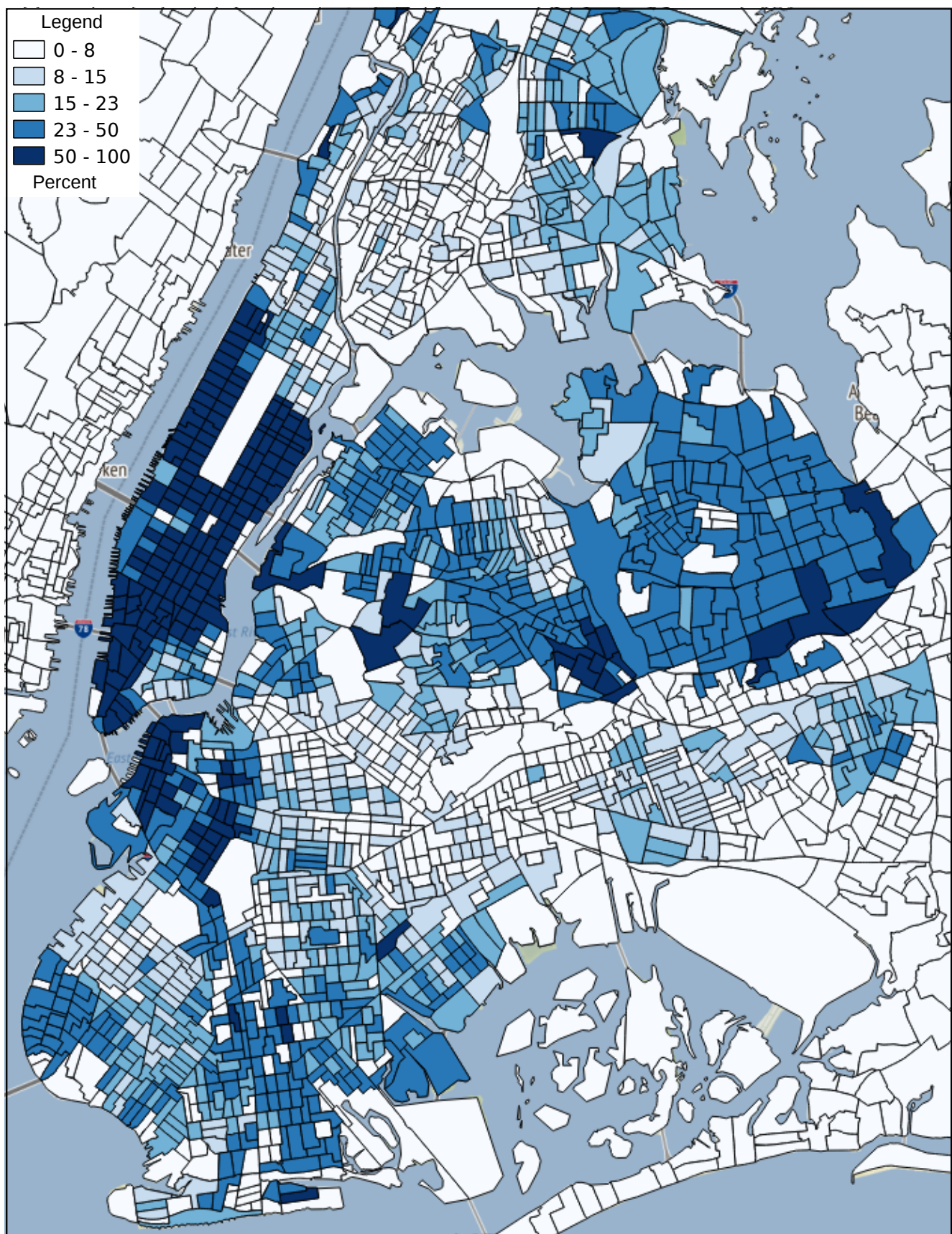


Figure S10. New York City: Share College Education 2000.

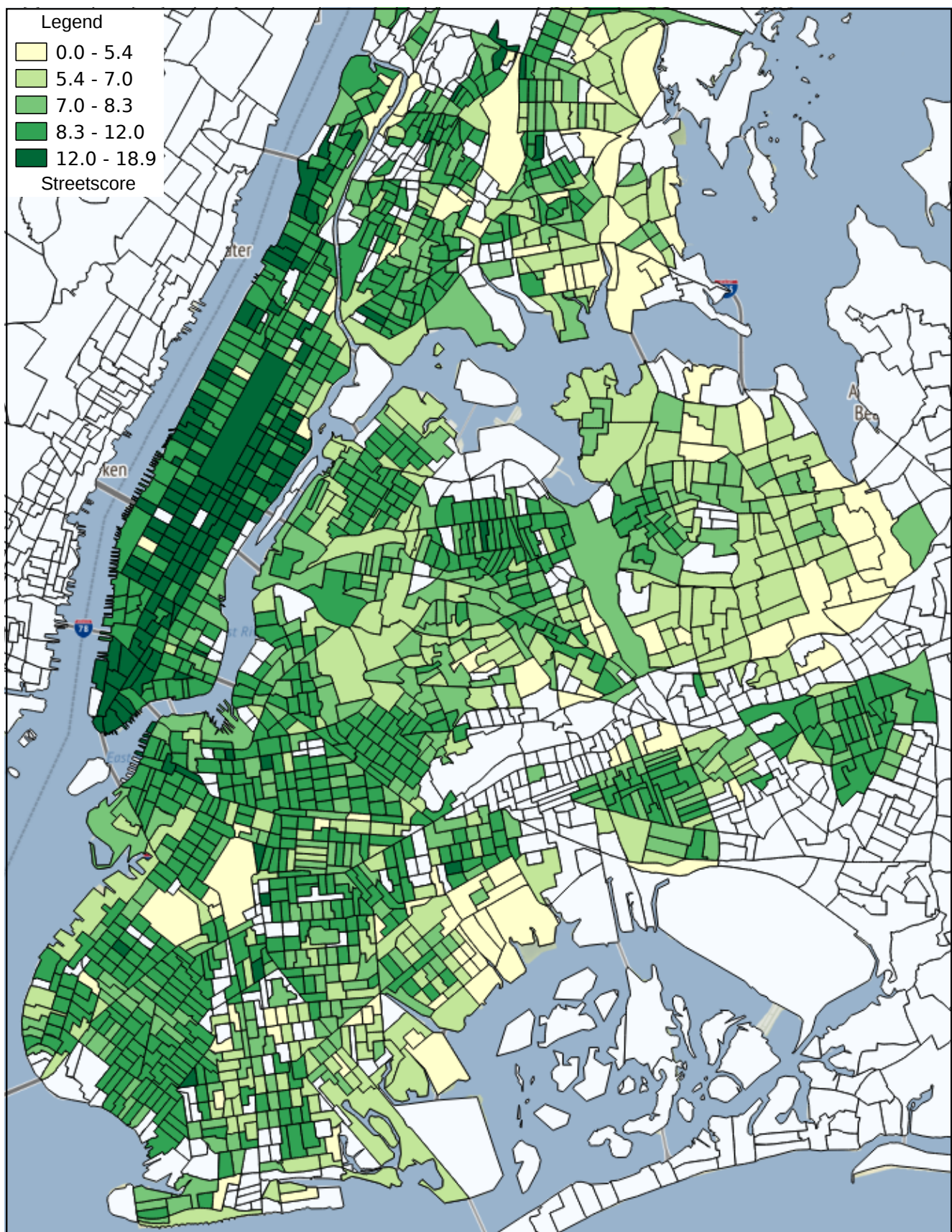


Figure S11. New York City: Streetscore 2007.

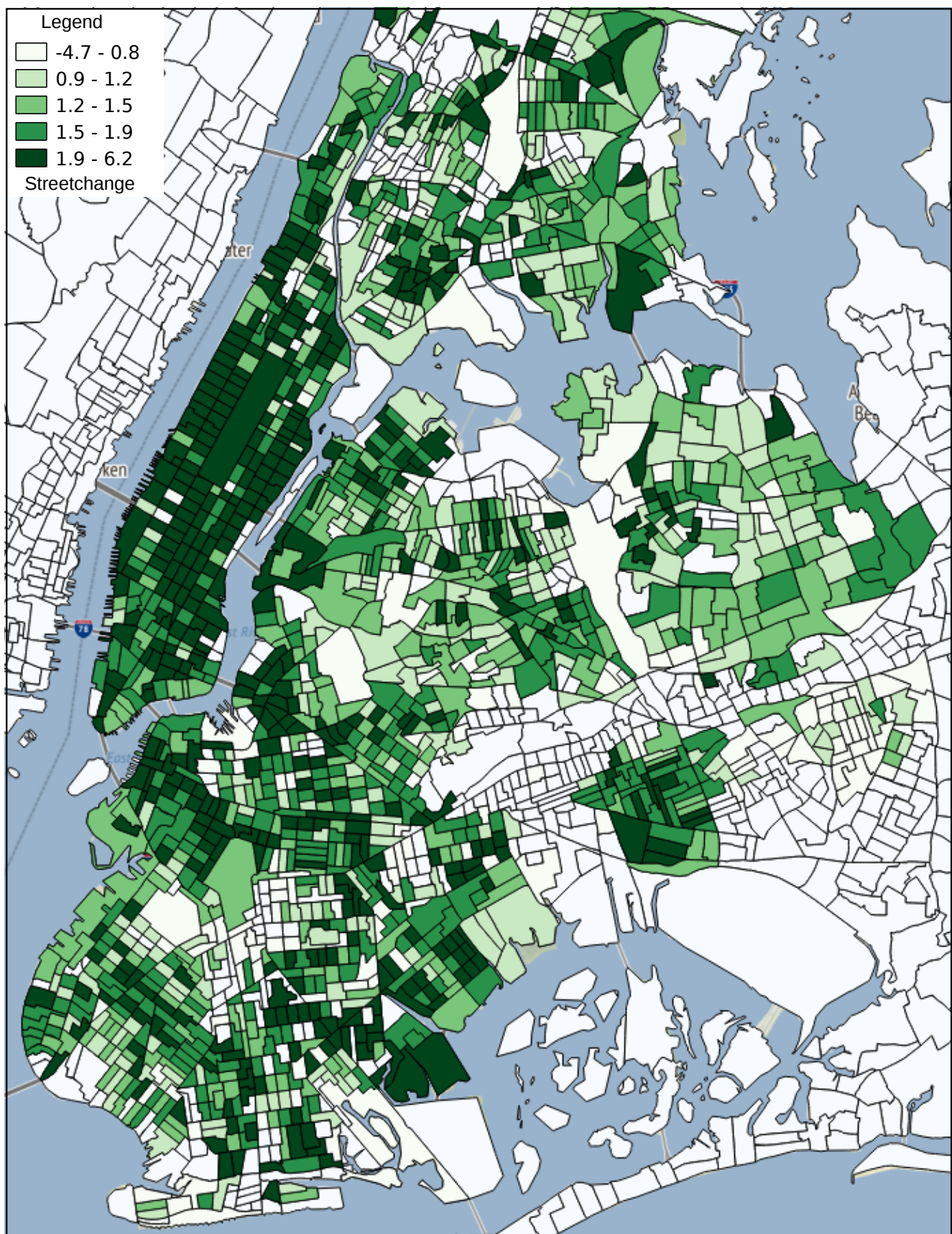


Figure S12. New York City: Streetchange 2007–2014.

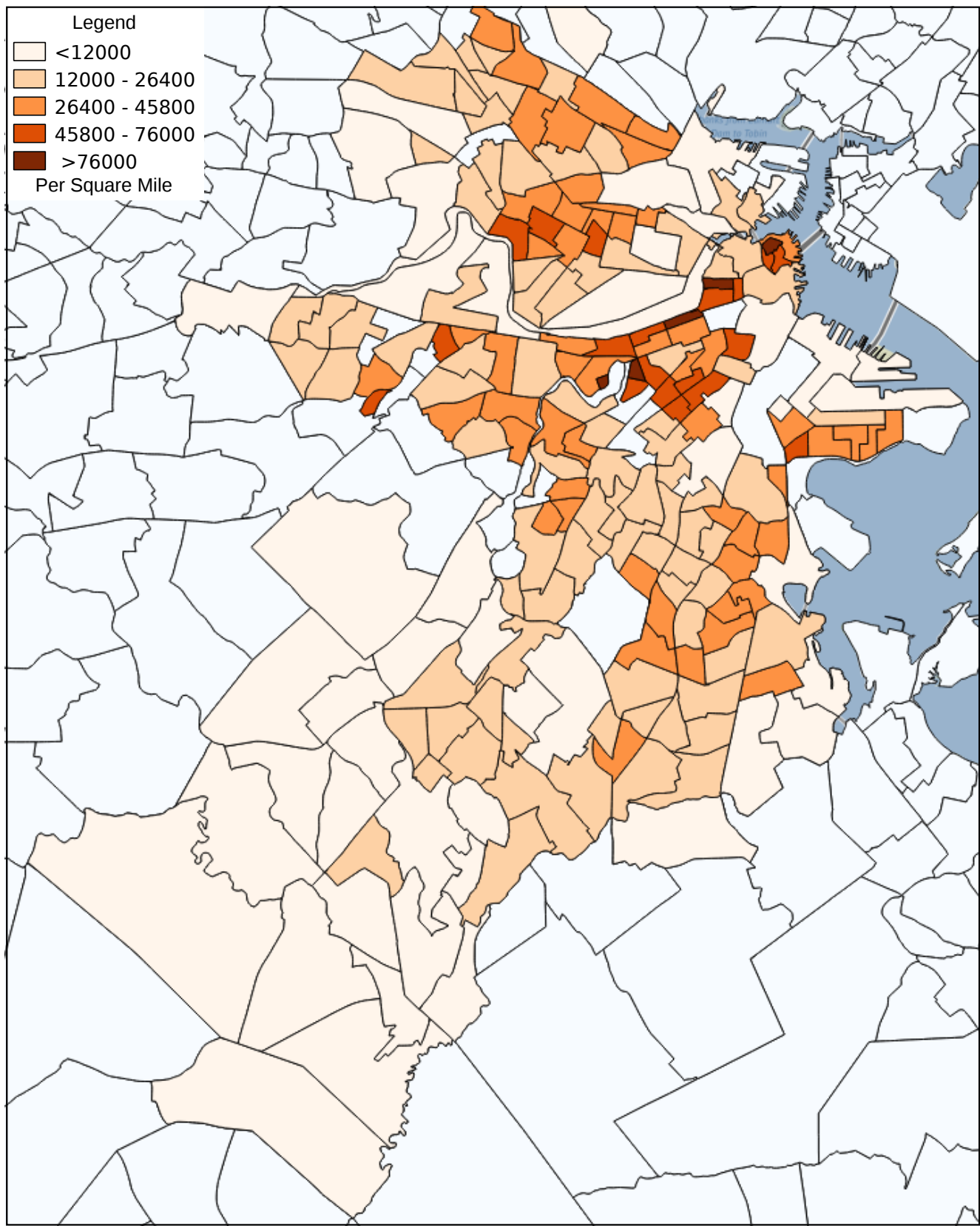


Figure S13. Boston: Log Population Density 2000.

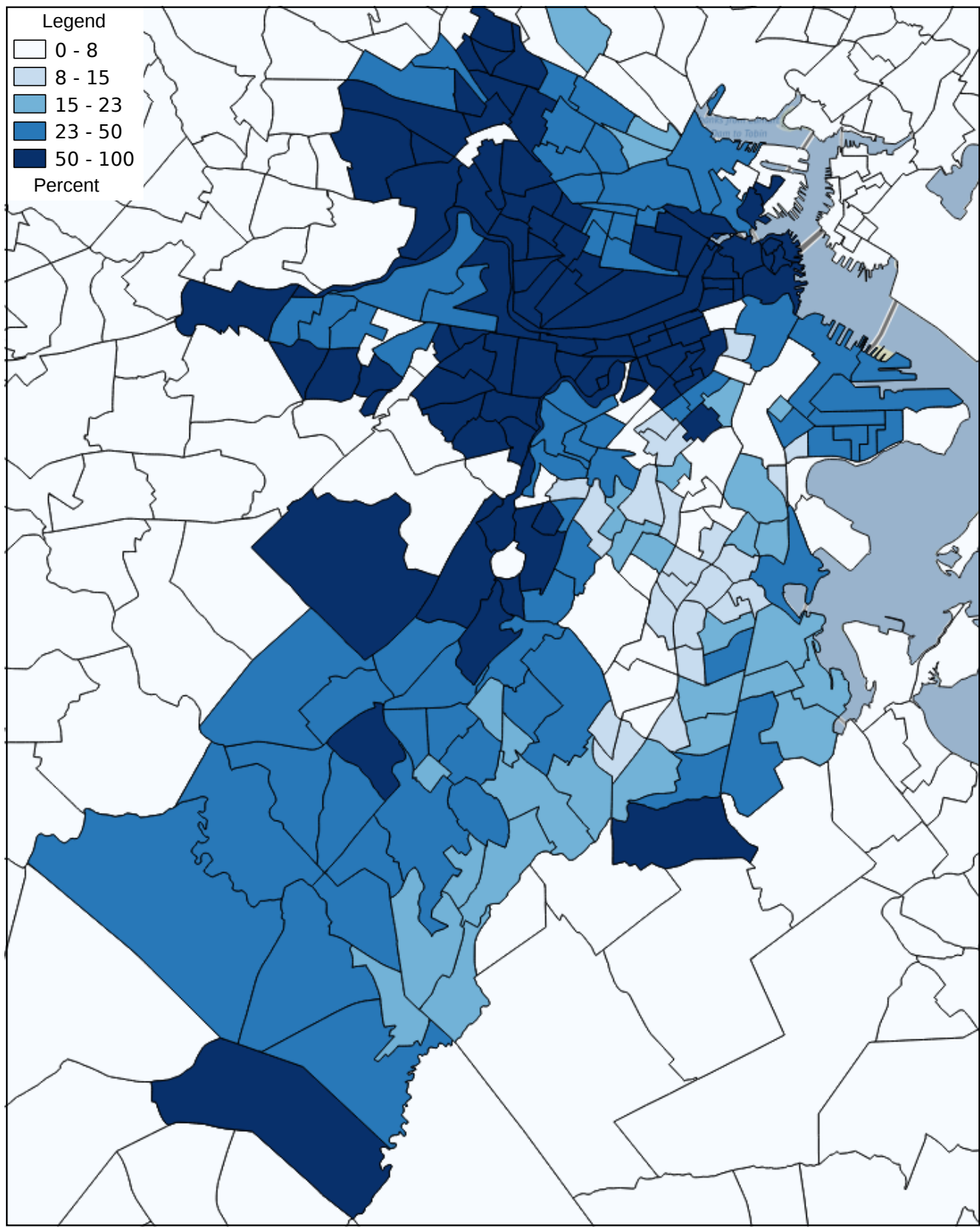


Figure S14. Boston: Share College Education 2000.

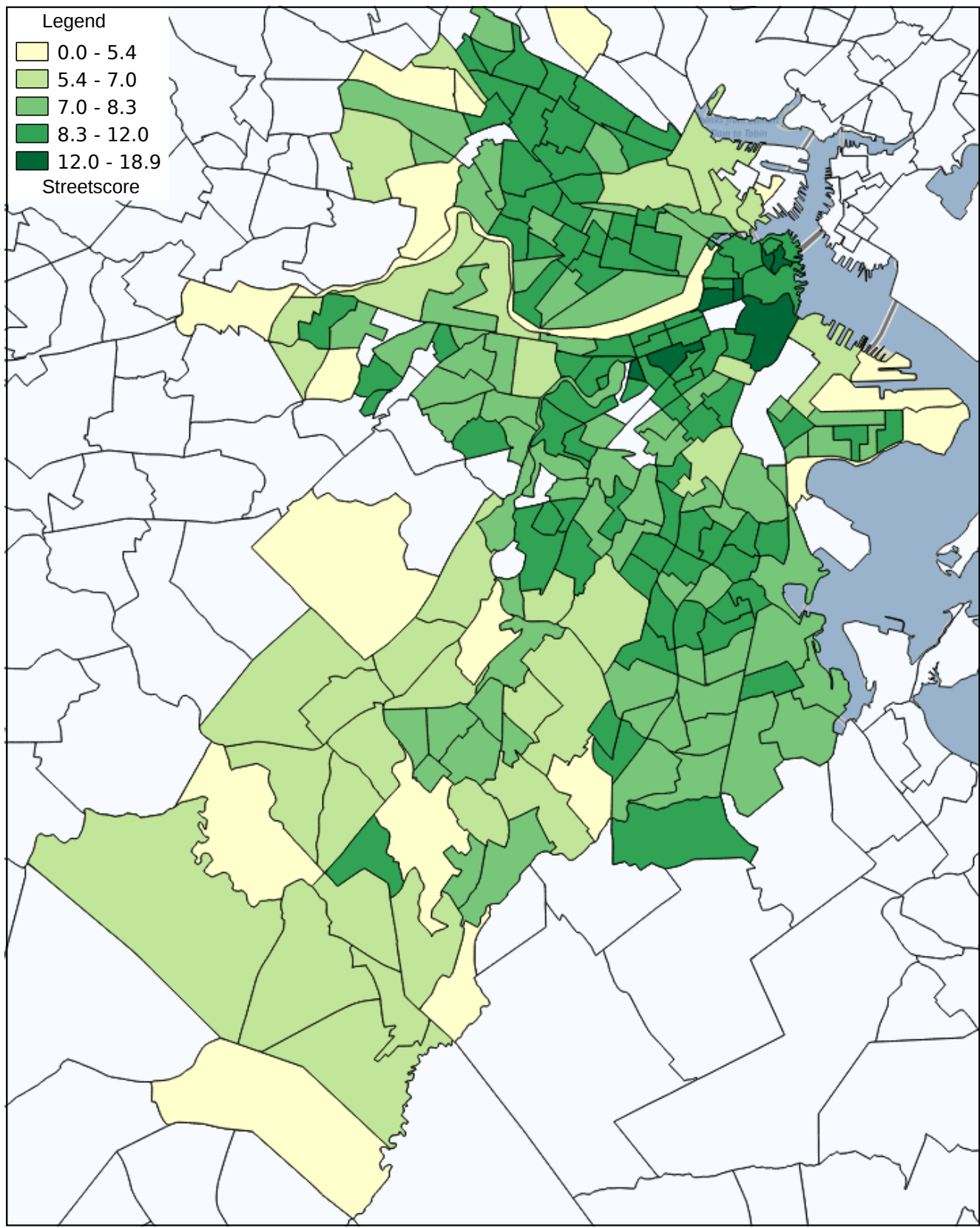


Figure S15. Boston: Streetscore 2007.

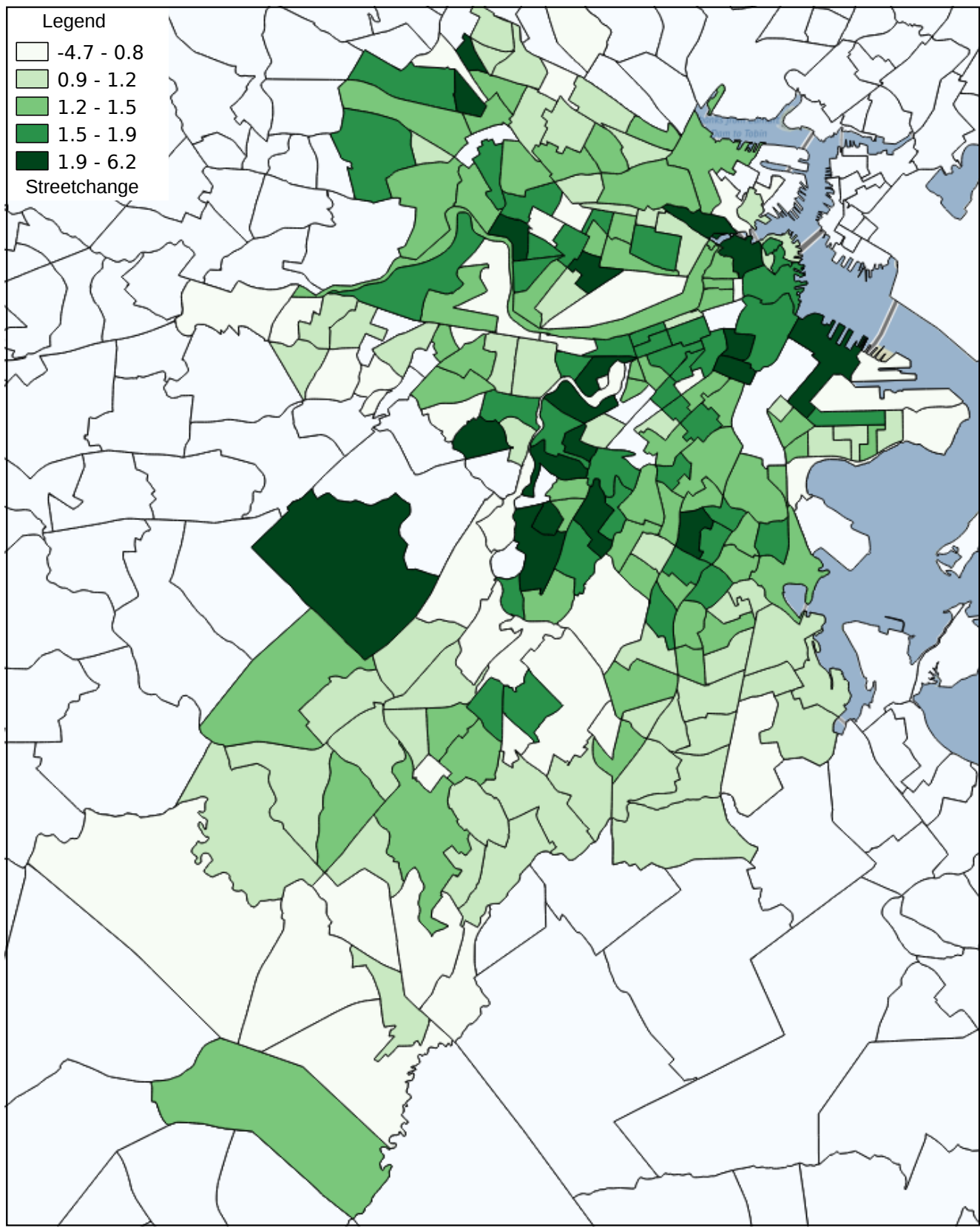


Figure S16. Boston: Streetchange 2007–2014.

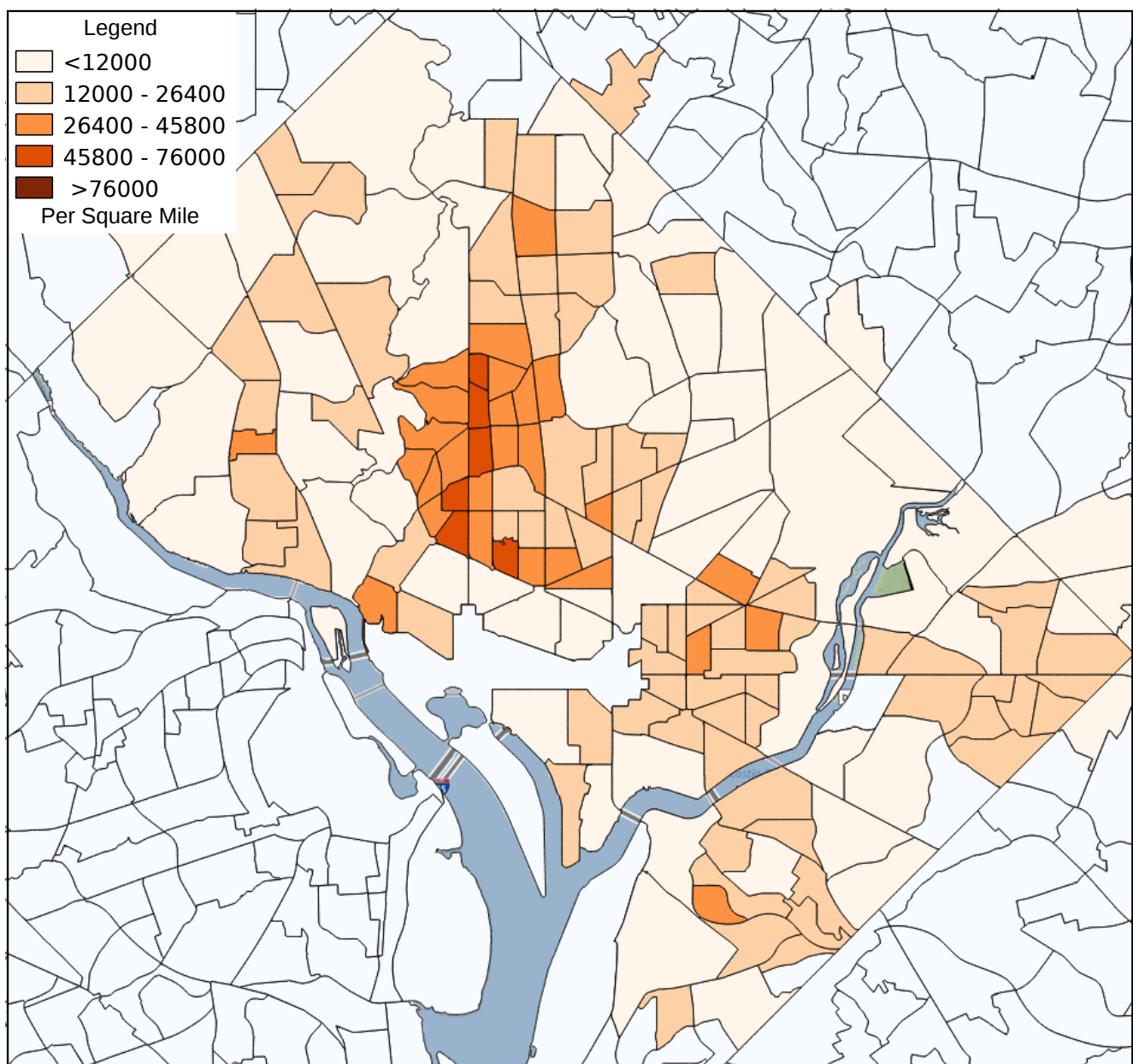


Figure S17. Washington DC: Log Population Density 2000.

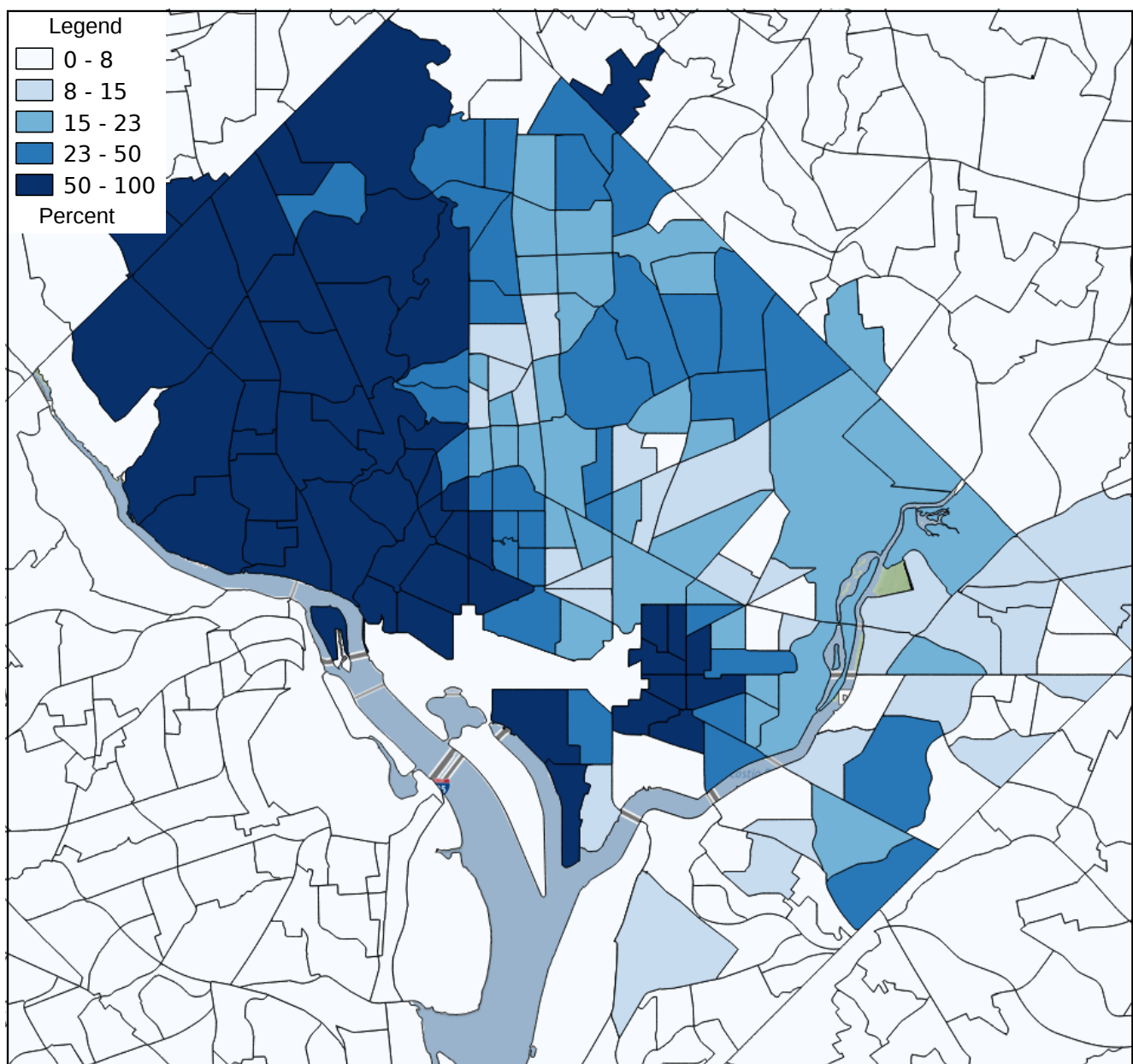


Figure S18. Washington DC: Share College Education 2000.

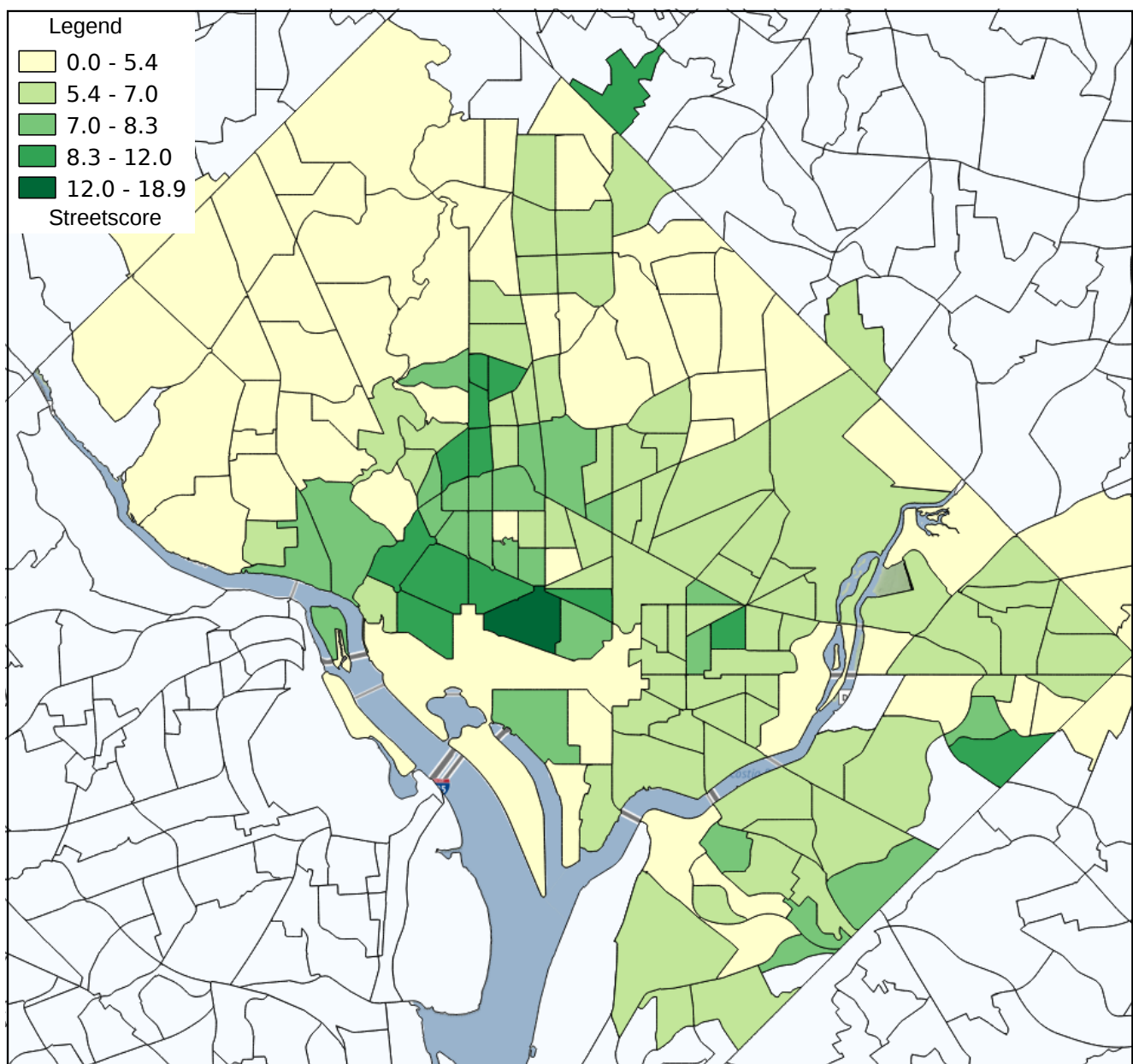


Figure S19. Washington DC: Streetscore 2007.

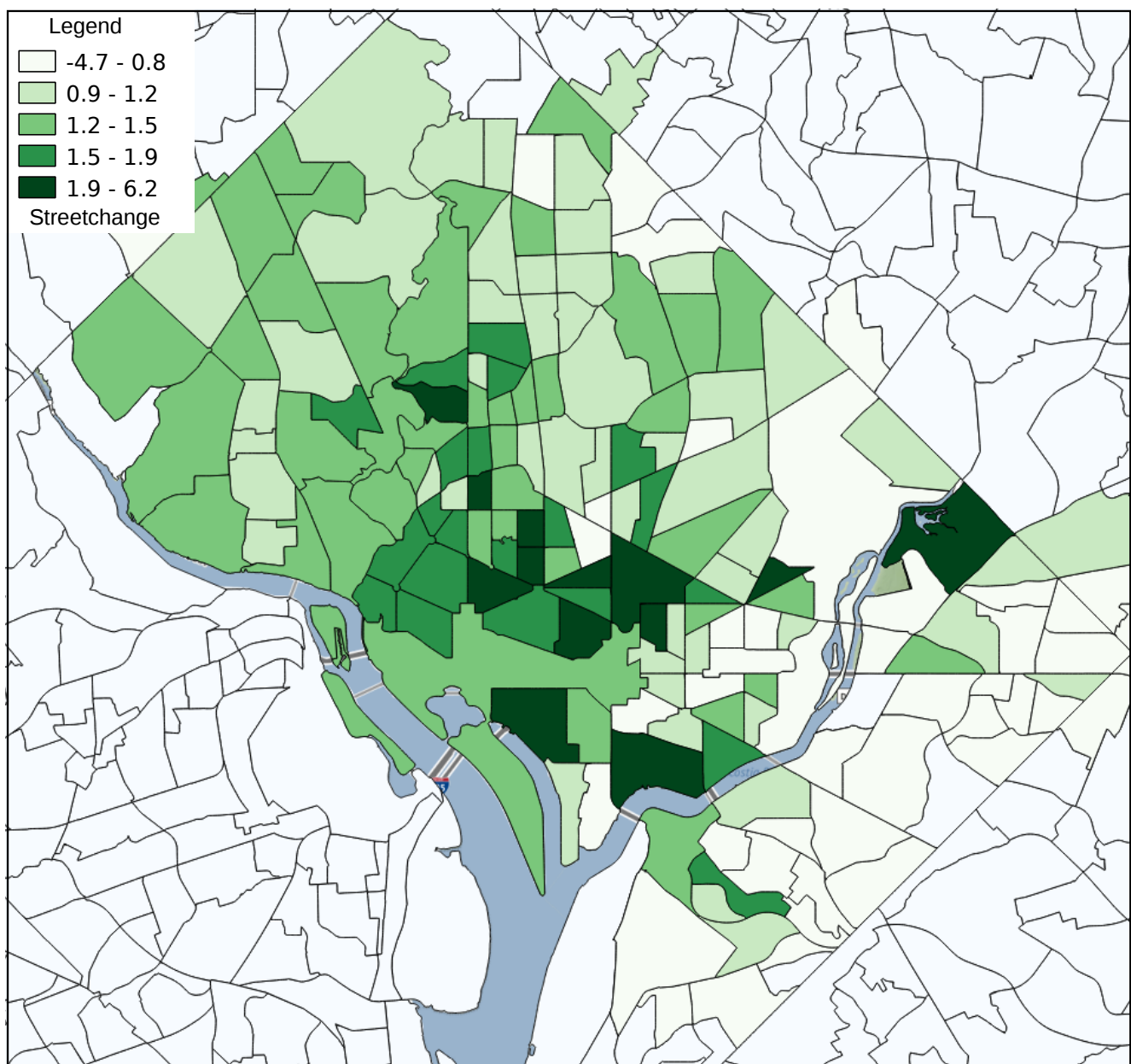


Figure S20. Washington DC: Streetchange 2007–2014.

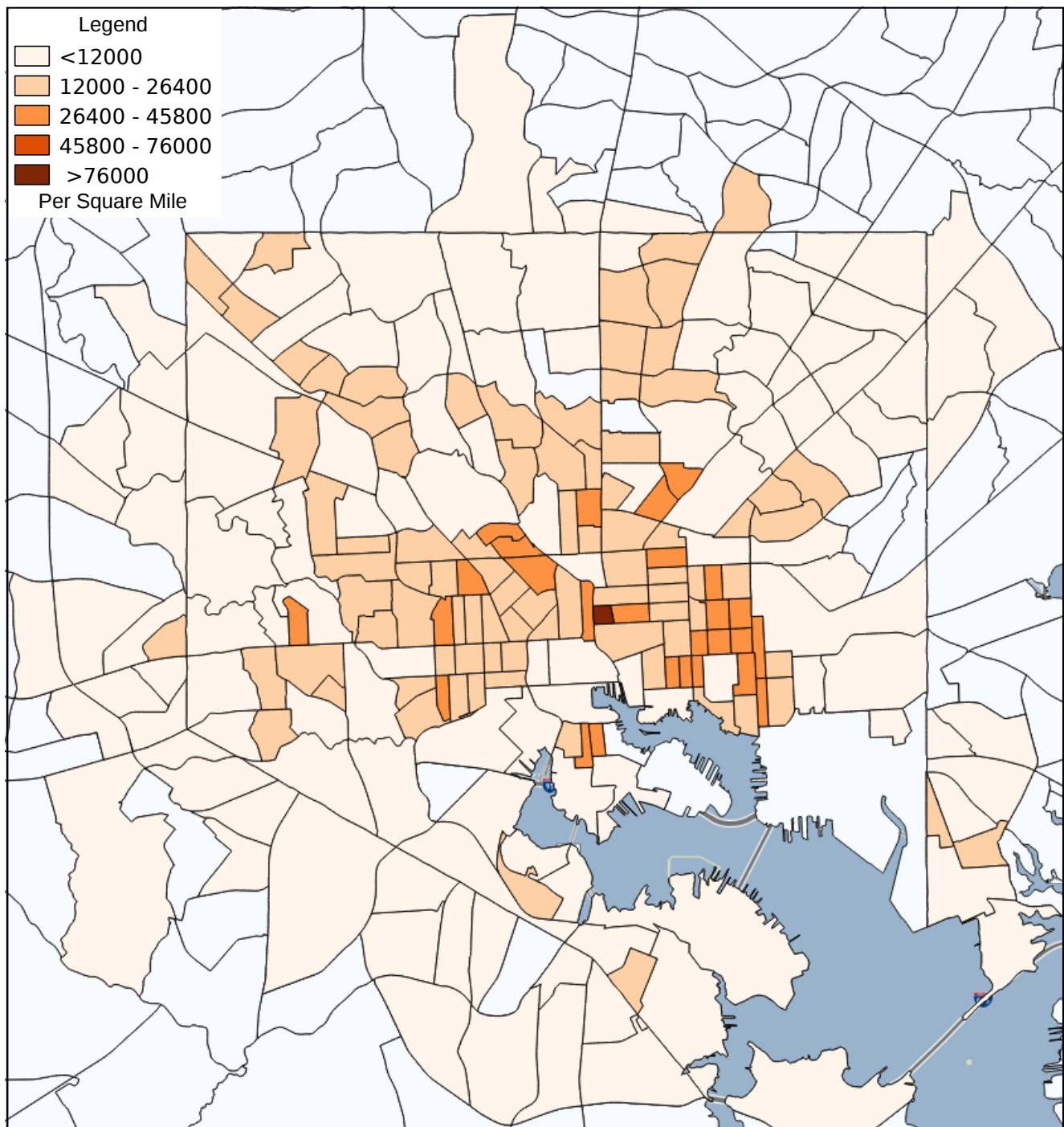


Figure S21. Baltimore: Log Population Density 2000.

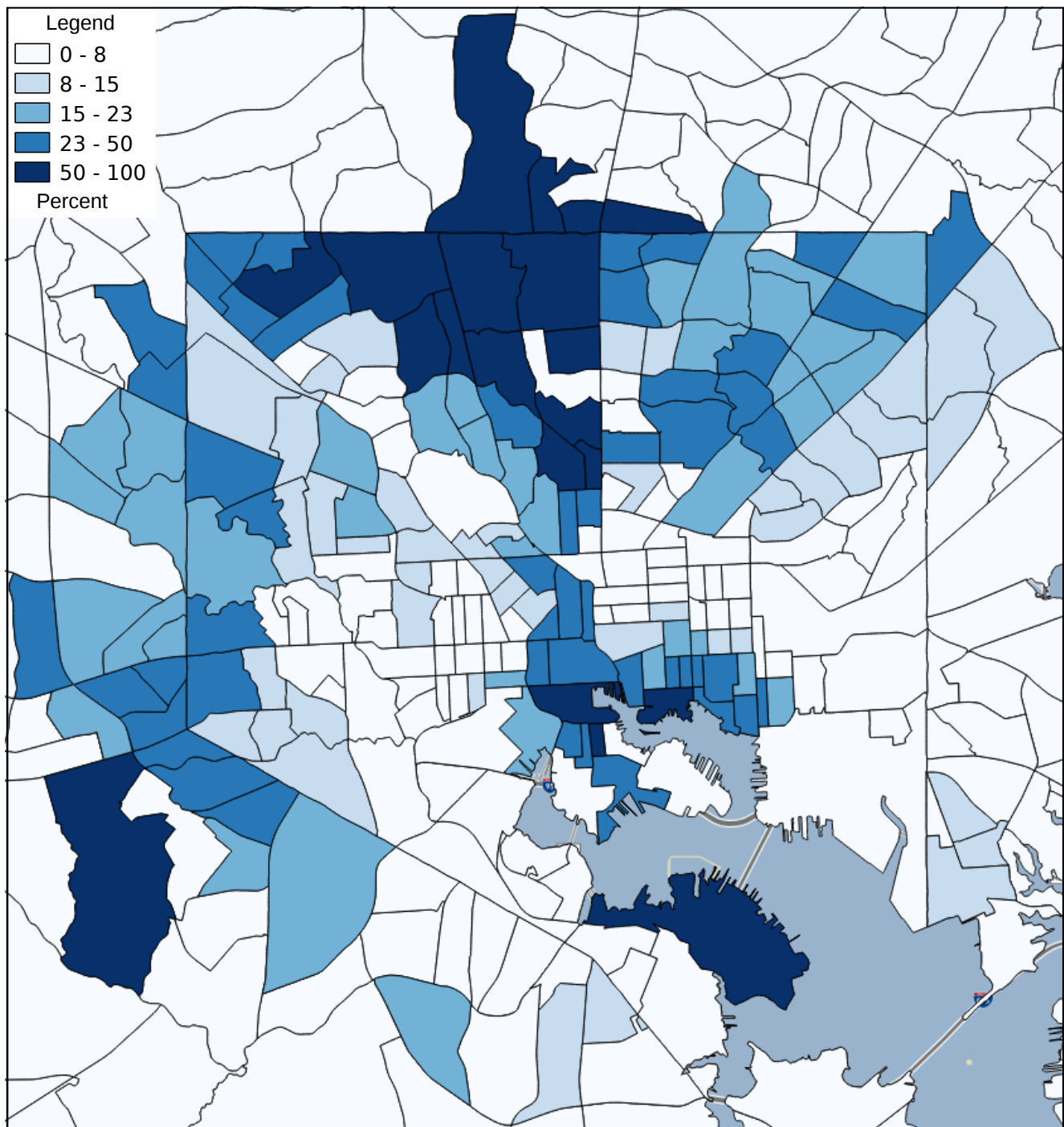


Figure S22. Baltimore: Share College Education 2000.

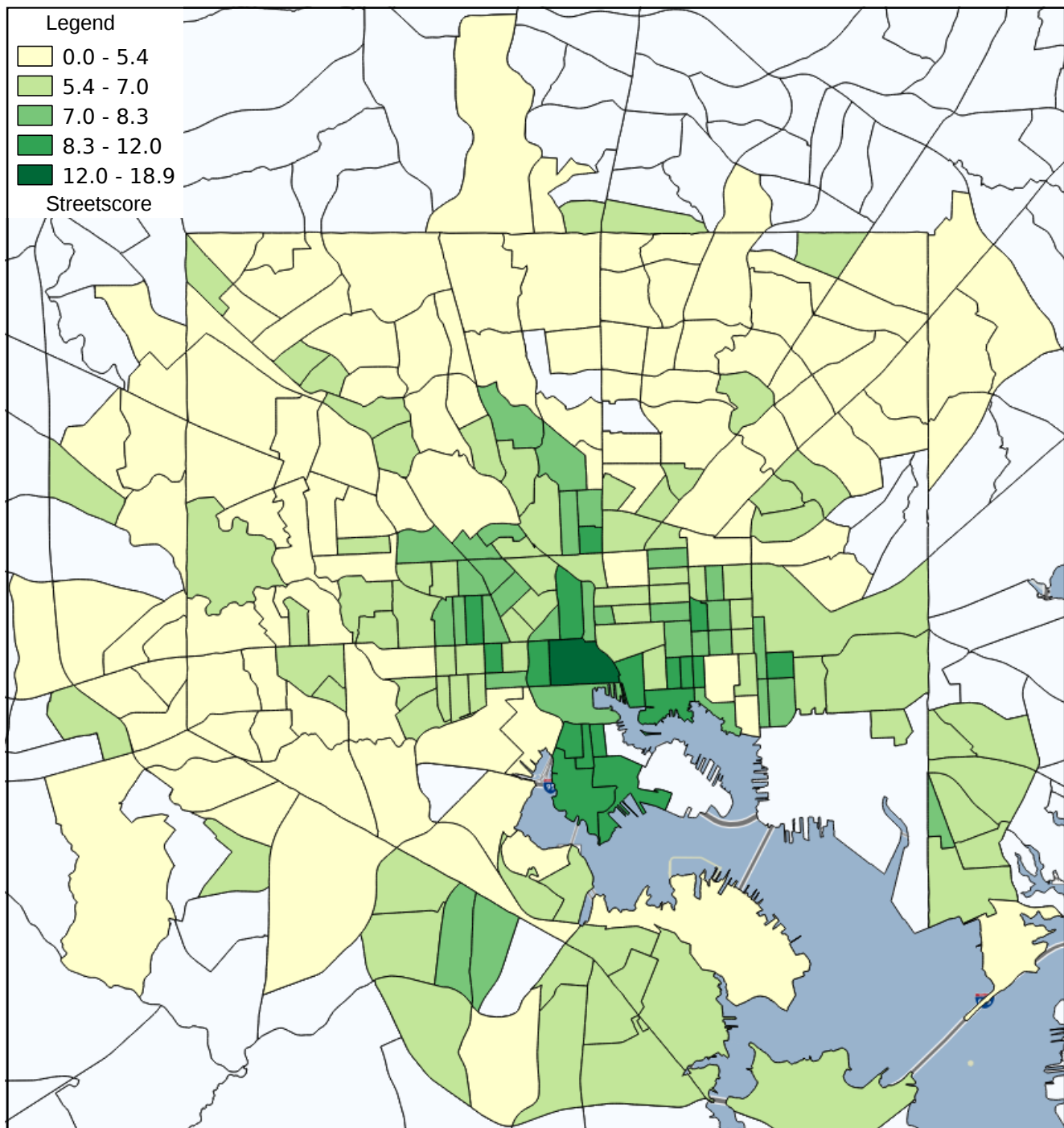


Figure S23. Baltimore: Streetscore 2007.

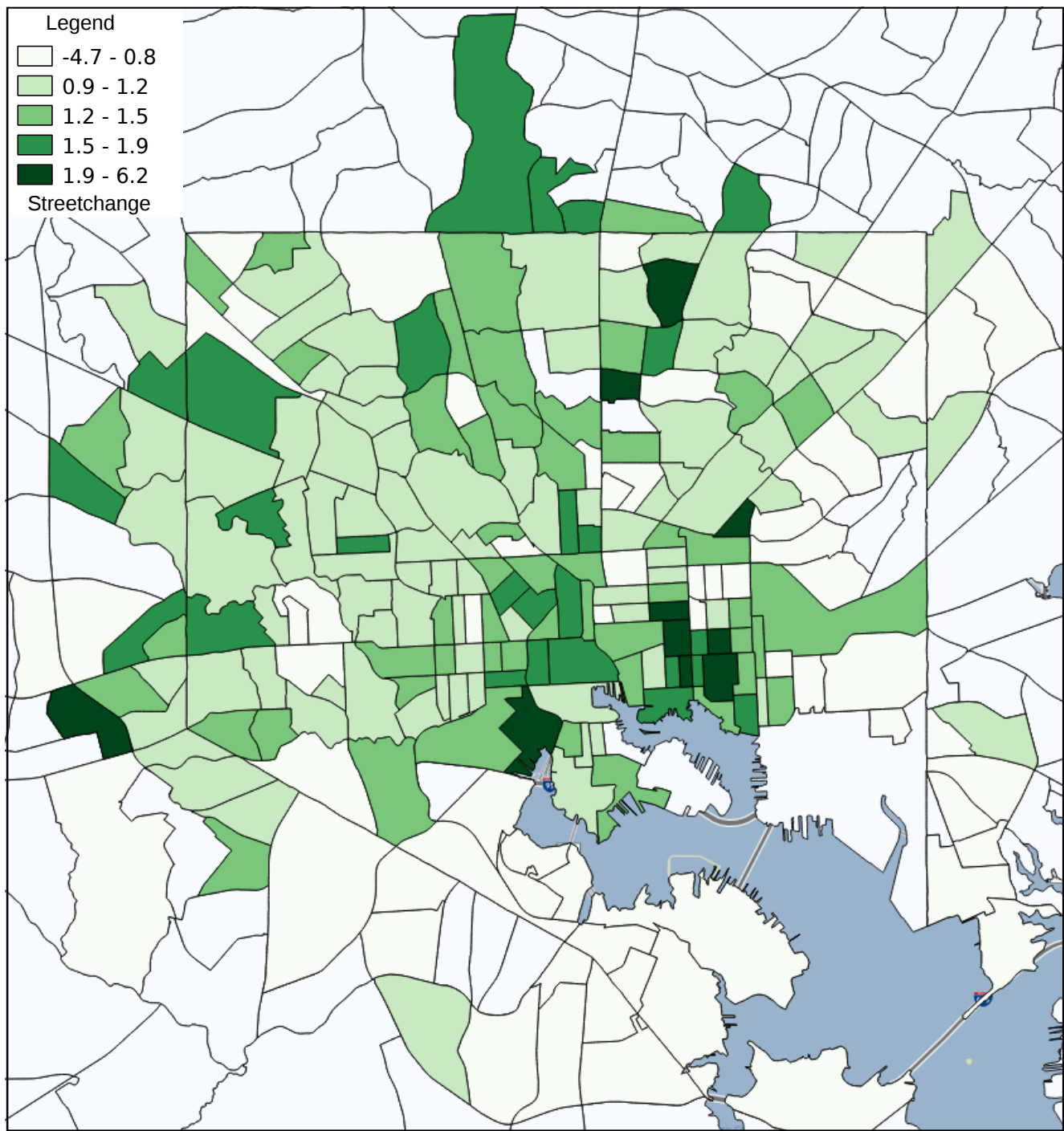


Figure S24. Baltimore: Streetchange 2007–2014.

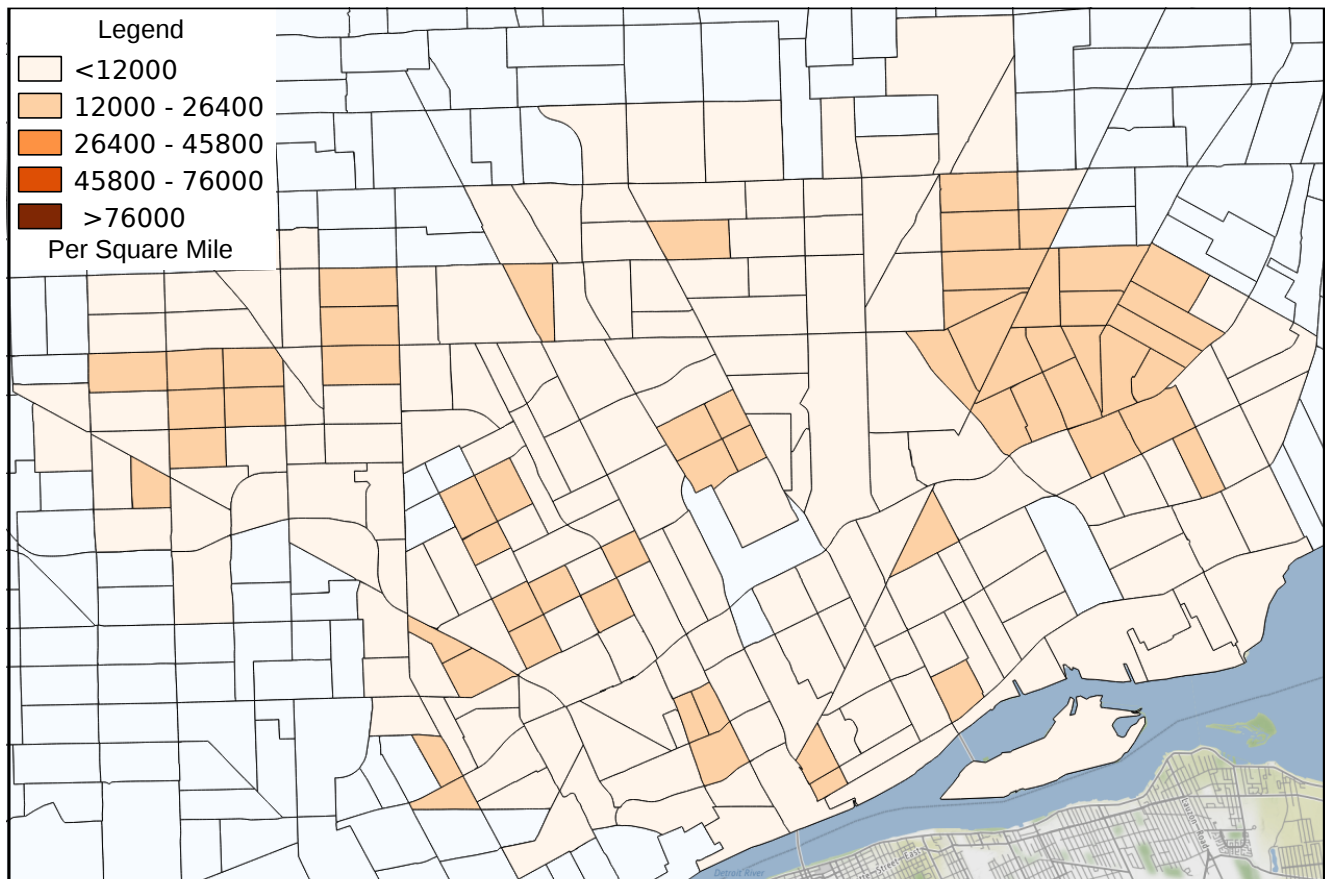


Figure S25. Detroit: Log Population Density 2000.

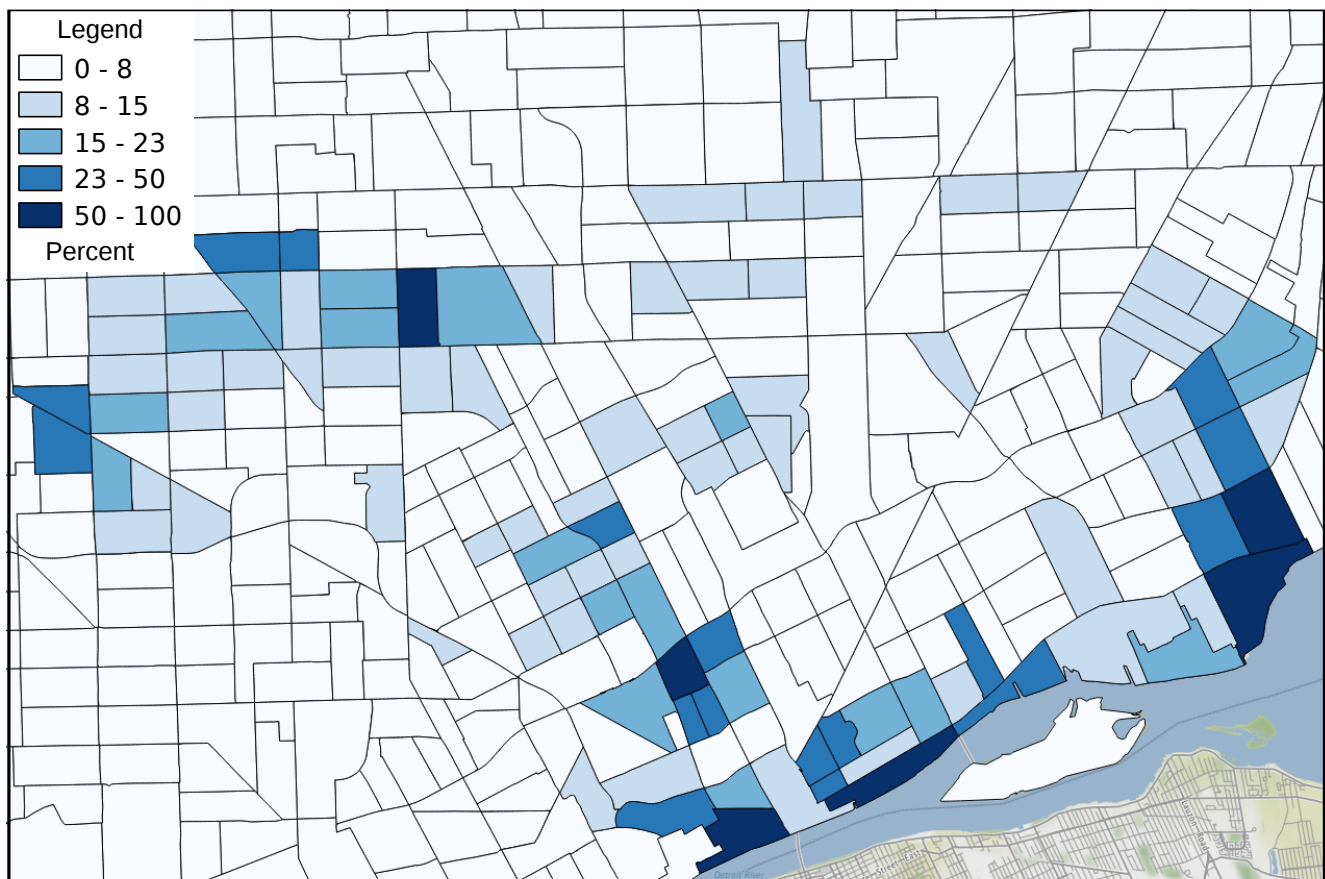


Figure S26. Detroit: Share College Education 2000.

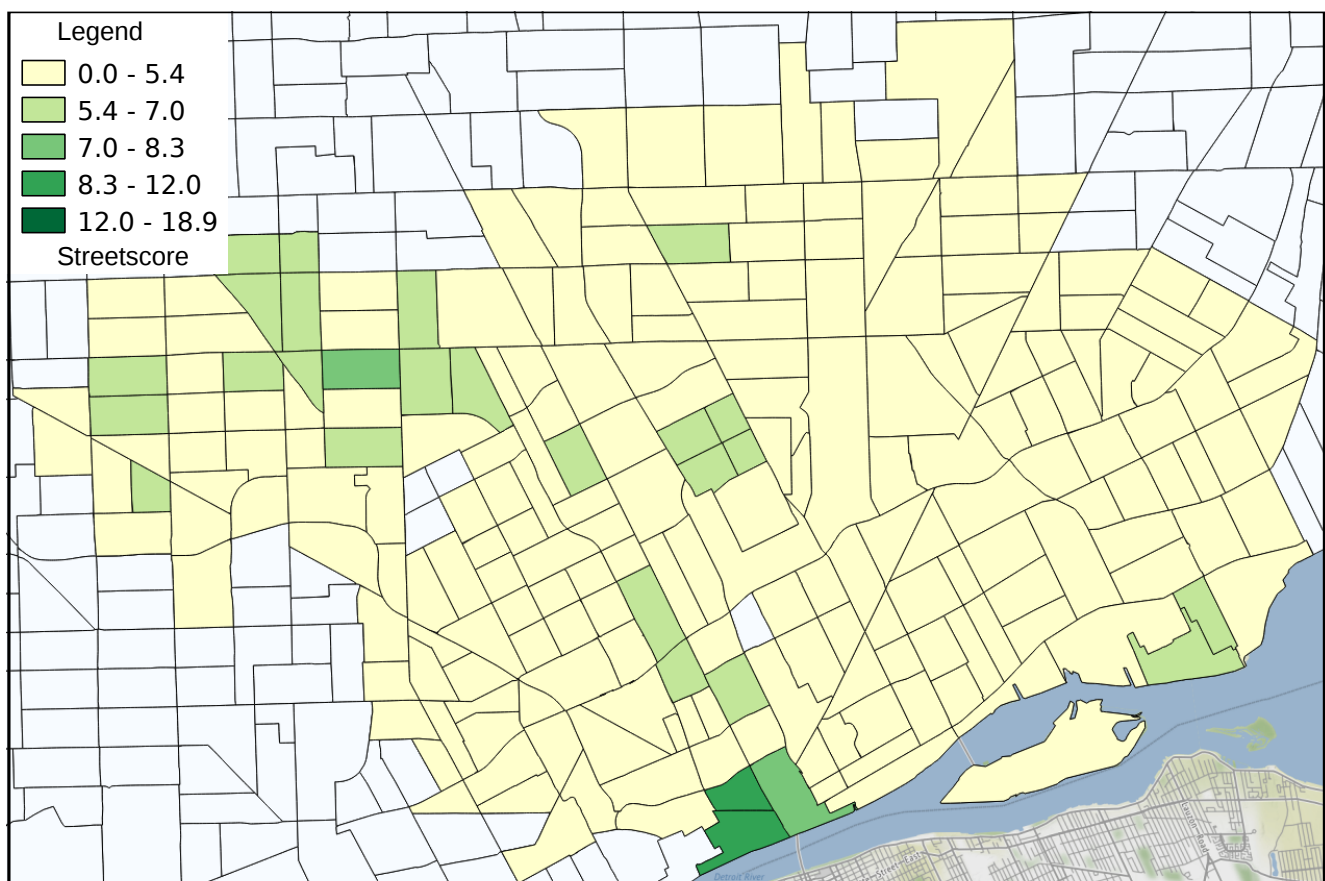


Figure S27. Detroit: Streetscore 2007.

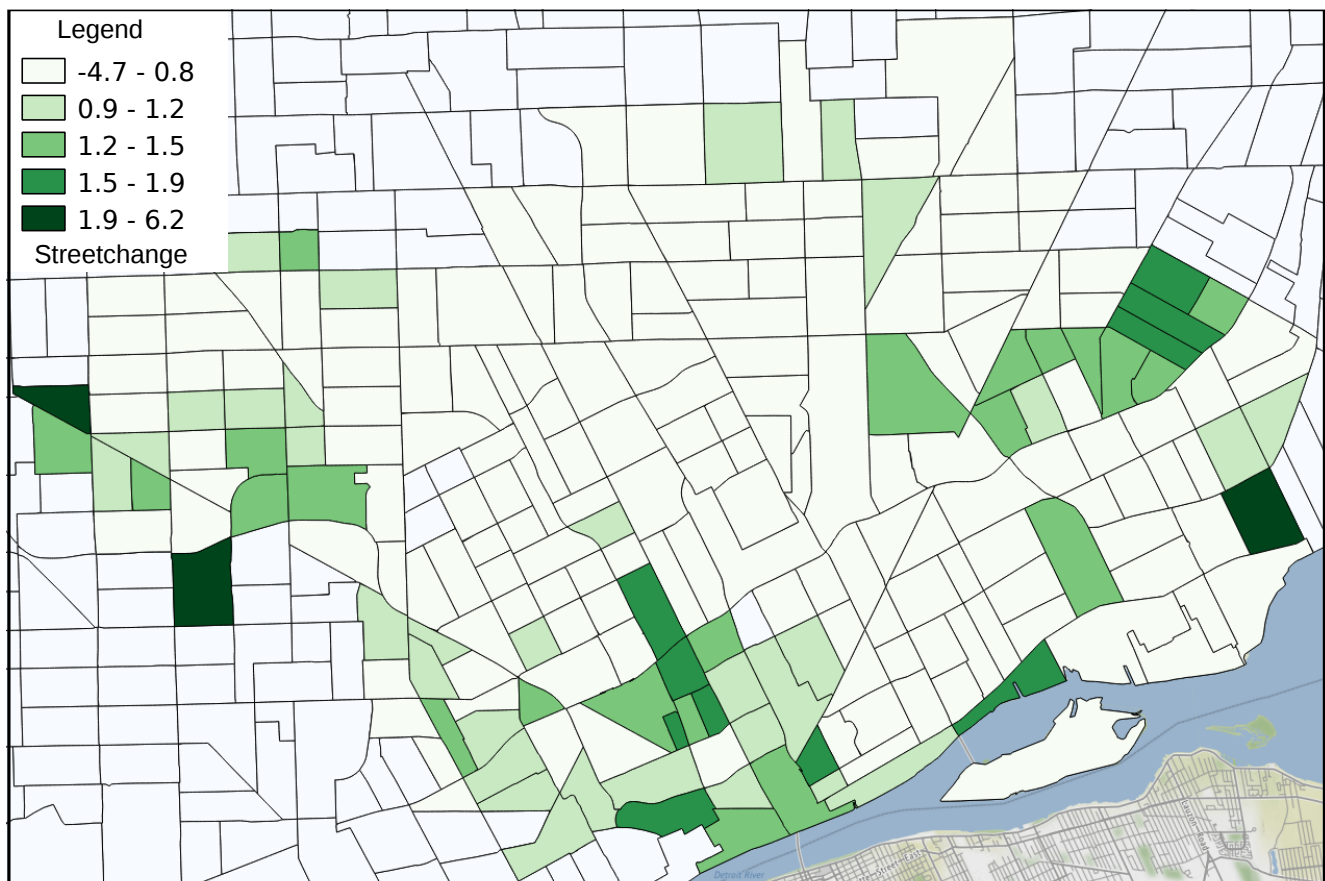


Figure S28. Detroit: Streetchange 2007–2014.